

# Approximating Maximum Independent Set for Rectangles in the Plane

Joseph S. B. Mitchell\*

December 23, 2024

## Abstract

We give a polynomial-time constant-factor approximation algorithm for maximum independent set for (axis-aligned) rectangles in the plane. Using a polynomial-time algorithm, the best approximation factor previously known is  $O(\log \log n)$ . The results are based on a new form of recursive partitioning in the plane, in which faces that are constant-complexity and orthogonally convex are recursively partitioned in a constant number of such faces.

## 1 Introduction

Given a set  $\mathcal{R} = \{R_1, \dots, R_n\}$  of  $n$  axis-aligned rectangles in the plane, the *maximum independent set of rectangles* (MISR) problem seeks a maximum-cardinality subset,  $\mathcal{R}^* \subseteq \mathcal{R}$ , of rectangles that are *independent*, meaning that any two rectangles of  $\mathcal{R}^*$  are interior-disjoint.

The MISR is an NP-hard ([12, 16]) special case of the fundamental Maximum Independent Set (MIS) optimization problem, in which, for a given input graph, one seeks a maximum-cardinality subset of its vertices such that no two vertices are joined by an edge. The MIS is an optimization problem that is very difficult to approximate, in its general form; the best polynomial-time approximation algorithm is an  $O(n/\log^2 n)$ -approximation [6], and there is no polynomial-time  $n^{1-\delta}$ -approximation algorithm, for any fixed  $\delta > 0$ , unless  $P=NP$  [21].

Because the MIS is such a challenging problem in its general setting, the MIS in special settings, particularly geometric settings, has been extensively studied. For string graphs (arcwise-connected sets), an  $n^\epsilon$ -approximation algorithm is known [13]. For outerstring graphs, a polynomial-time exact algorithm is known [17], provided a geometric representation of the graph is given. For geometric objects that are “fat” (e.g., disks, squares), a Polynomial-Time Approximation Scheme (PTAS) is known [11]. Fatness is critical in many geometric approximation settings. The MISR is one of the most natural geometric settings for MIS in which the objects are *not* assumed to be fat – rectangles can have arbitrary aspect ratios. The MISR arises naturally in various applications, including resource allocation, data mining, and map labeling.

For the MISR, the celebrated results of Adamaszek, Har-Peled, and Wiese [1, 2, 3, 15] give a *quasipolynomial*-time approximation scheme, yielding a  $(1 - \epsilon)$ -approximation in time  $n^{\text{poly}(\log n/\epsilon)}$ . Chuzhoy and Ene [9] give an improved, but still not polynomial, running time: they present a  $(1 - \epsilon)$ -approximation algorithm with a running time of  $n^{O((\log \log n/\epsilon)^4)}$ . Recently, Grandoni, Kratsch, and Wiese [14] give a parameterized approximation scheme, which, for given  $\epsilon > 0$  and integer  $k > 0$ , takes time  $f(k, \epsilon)n^{g(\epsilon)}$  and either outputs a solution of size  $\geq k/(1 + \epsilon)$  or determines that the optimum solution has size  $< k$ .

Turning now to *polynomial*-time approximation algorithms for MISR, early algorithms achieved an approximation ratio of  $O(\log n)$  [4, 18, 20] and  $\lceil \log_k n \rceil$ , for any fixed  $k$  [5]. In a significant breakthrough, the  $O(\log n)$  approximation bound was improved to  $O(\log \log n)$  [8, 7], which has remained the best approximation factor during the last decade. Indeed, it has been a well known open problem to improve on

---

\*Stony Brook University, Stony Brook, NY 11794-3600, joseph.mitchell@stonybrook.edu

this approximation factor: “even for the axis-parallel rectangles case currently has no constant factor approximation algorithm in polynomial time” [1], and “obtaining a PTAS, or even an efficient constant-factor approximation remains elusive for now” [9].

## Our Contribution

We give a polynomial-time  $O(1)$ -approximation algorithm for MISR, improving substantially on the prior  $O(\log \log n)$  approximation factor for a polynomial-time algorithm. The algorithm is based on a novel means of recursively decomposing the plane, into constant-complexity (orthogonally convex) “corner-clipped rectangles” (CCRs), such that any set of disjoint (axis-aligned) rectangles has a constant-fraction subset that “nearly respects” the decomposition, in a manner made precise below. The fact that the CCRs are of constant complexity, and the partitioning recursively splits a CCR into a constant number of CCRs, allow us to give an algorithm, based on dynamic programming, that computes such a subdivision, while maximizing the size of the subset of  $\mathcal{R}$  of rectangles that are not penetrated (in their interiors) by the cuts. Together, the structure theorem and the dynamic program, imply the result.

Two key ideas are used in obtaining our result: (1) instead of a recursive partition based on a binary tree, partitioning each problem into two subproblems, we utilize a  $K$ -ary partition, with constant  $K \leq 5$ ; (2) instead of subproblems based on rectangles (arising from axis-parallel cuts), we allow more general cuts, which are constant-complexity planar graphs having edges defined by axis-parallel segments, with resulting regions being orthogonally convex (CCR) faces of constant complexity. Proof of our structural theorem relies on a key idea to use maximal expansions of an input set of rectangles, enabling us to classify rectangles of an optimal solution in terms of their “nesting” properties with respect to abutting maximal rectangles. This sets up a charging scheme that can be applied to a subset of at least half of the maximal expansions of rectangles in an optimal solution: those portions of cuts that cross these rectangles can be accounted for by means of a charging scheme, allowing us to argue that a constant fraction subset of original rectangles exists that (nearly) respects a recursive partitioning into CCRs. These properties then enable a dynamic programming algorithm to achieve a constant factor approximation in polynomial time.

## 2 Preliminaries

Throughout this paper, when we refer to a rectangle we mean an *axis-aligned*, closed rectangle in the plane. We let  $[x, x'] \times [y, y']$  denote the rectangle whose projection on the  $x$ -axis (resp.,  $y$ -axis) is the (closed) interval  $[x, x']$  (resp.,  $[y, y']$ ). We often speak of the *sides* (or *edges*) of a rectangle; we consider each rectangle to have four sides (top, bottom, left, right), each of which is a closed (horizontal or vertical) line segment. Two nonparallel sides of a rectangle meet at a common endpoint, one of the *corners* of the rectangle, often distinguished as being northeast, northwest, southwest, or southeast. When we speak of rectangles being disjoint, we mean that their interiors are disjoint. We say that two rectangles *abut* (or *are in contact*) if their interiors are disjoint, but there is an edge of one rectangle that has a nonzero-length overlap with an edge of the other rectangle. We say that a horizontal/vertical line segment  $\sigma$  *penetrates* a rectangle  $R \in \mathcal{R}$  if  $\sigma$  intersects the interior of  $R$ . We say that a horizontal/vertical line segment  $\sigma$  *crosses* another horizontal/vertical segment  $\sigma'$  if the two segments intersect in a point that is interior to both segments; similarly, we say that  $\sigma$  *crosses* a rectangle  $R$  if the intersection  $\sigma \cap R$  is a subsegment of  $\sigma$  that is interior to  $\sigma$ .

The input to our problem is a set  $\mathcal{R}$  of  $n$  arbitrarily overlapping (axis-aligned) rectangles in the plane. Without loss of generality, we can assume that the  $x$ -coordinates and  $y$ -coordinates that define the rectangles  $\mathcal{R}$  are distinct and are integral. Let  $x_1, x_2, \dots, x_{2n}$ , with  $x_1 < x_2 < \dots < x_{2n}$ , be the sorted  $x$ -coordinates of the left/right sides of the  $n$  input rectangles  $\mathcal{R}$ ; similarly, let  $y_1 < y_2 < \dots < y_{2n}$  be the  $y$ -coordinates of the top/bottom sides of the input. We let  $BB(\mathcal{R}) = [x_1, x_{2n}] \times [y_1, y_{2n}]$  denote the axis-aligned bounding box (minimal enclosing rectangle) of the rectangles  $\mathcal{R}$ . The arrangement of the horizontal/vertical lines ( $x = x_i$ ,  $y = y_j$ ) that pass through the sides of the rectangles  $\mathcal{R}$  determine a *grid*  $\mathcal{G}$ , with faces (rectangular grid cells), edges (line segments along the defining lines), and vertices (at points where the defining lines cross).

In the maximum independent set of rectangles (MISR) problem on  $\mathcal{R}$  we seek a subset,  $\mathcal{R}^* \subseteq \mathcal{R}$ , of maximum cardinality,  $k^* = |\mathcal{R}^*|$ , such that the rectangles in  $\mathcal{R}^*$  are *independent* in that they have pairwise disjoint interiors. Our main result is a polynomial-time algorithm to compute an independent subset of  $\mathcal{R}$  of cardinality  $\Omega(k^*)$ .

**Corner-Clipped Rectangles (CCRs).** An *orthogonal polygon* is a simple polygon<sup>1</sup> whose boundary consists of a finite set of axis-parallel segments. A *corner-clipped rectangle*  $Q$  is a special orthogonal polygon obtained by removing a set of up to four disjoint subrectangles from a given rectangle  $R$ , with each subrectangle containing exactly one of the four corners of  $R$ . More precisely, for a given rectangle  $R$  and a (possibly empty) set  $\{R_{NE}, R_{NW}, R_{SW}, R_{SE}\}$  of up to four disjoint rectangles, each containing exactly one corner (vertex) of  $R$  in its interior, a corner-clipped rectangle  $Q$  is given by subtracting from  $R$  the interiors of the corner-covering rectangles  $R_i$ , so that  $Q = R \setminus (\text{int}(R_{NE}) \cup \dots \cup \text{int}(R_{SE}))$ , where  $\text{int}(\cdot)$  denotes interior. Note that a CCR  $Q$  is an orthogonally convex (orthogonal) polygon: any horizontal or vertical line that intersects it intersects it in a connected set (a horizontal or vertical line segment). CCRs include rectangles, “L-shaped” regions, “T-shaped” regions, “+ -shaped” regions, etc. A CCR has constant complexity, with at most 12 edges/vertices. Refer to Figure 1.

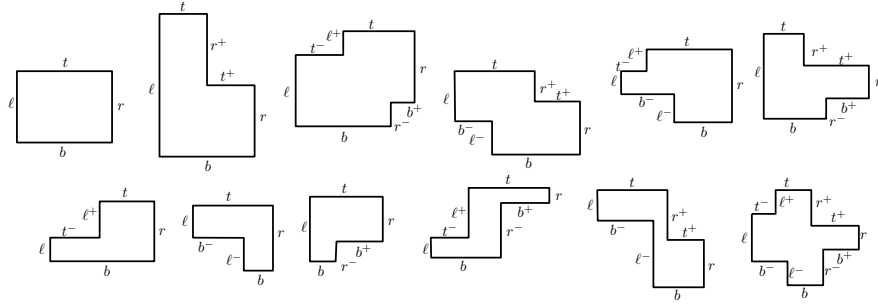


Figure 1: Examples of corner-clipped rectangles (CCRs).

Consider a CCR,  $Q$ . It has up to 3 (vertical) left sides (edges), which we label  $\ell$  (for the leftmost side, shared with the bounding box,  $BB(Q)$ ),  $\ell^+$  (for the side associated with a northwest clipping rectangle,  $R_{NEW}$ , if there is one), and  $\ell^-$  (for the side associated with southwest clipping rectangle,  $R_{SW}$ , if there is one). Similarly,  $Q$  has up to 3 (vertical) right sides ( $r$ ,  $r^+$ , and  $r^-$ ) up to 3 (horizontal) top sides ( $t$ ,  $t^+$ , and  $t^-$ ), and up to 3 (horizontal) bottom sides ( $b$ ,  $b^+$ , and  $b^-$ ). Refer to the edge labels in Figure 1.

**Maximal rectangles.** Let  $I$  be an independent set of rectangles within the bounding box  $BB(\mathcal{R})$ . We say that the set  $I$  is *maximal within*  $BB(\mathcal{R})$  if each rectangle  $R \in I$  has all four of its sides in nonzero-length contact with a side of another rectangle of  $I$ , or with the boundary of  $BB(\mathcal{R})$ . An arbitrary independent subset  $I = \{R_1, \dots, R_k\} \subseteq \mathcal{R}$  of input rectangles  $R_i$  can be converted into an independent set of rectangles,  $R'_i \supseteq R_i$ , that are maximal within  $B$ , in any of a number of ways, “expanding” each  $R_i$  appropriately. (Note that the super-rectangles,  $R'_i$  need not be elements of the input set  $\mathcal{R}$ .) To be specific, we define  $I' = \{R'_1, \dots, R'_k\}$  to be the set of *maximal expansions*,  $R'_i \supseteq R_i$ , of the rectangles  $R_i$ , obtained from the following process: Within the bounding box  $B$ , we extend each rectangle  $R_i$  upwards (in the  $+y$  direction) until it contacts another rectangle of  $I$  or contacts the top edge of  $BB(\mathcal{R})$ . We then extend these rectangles leftwards, then downwards, and then rightwards, in a similar fashion. This results in a new set  $I'$  of independent rectangles within  $BB(\mathcal{R})$ , with each rectangle  $R'_i$  containing the corresponding rectangle  $R_i$ , and each being maximal within the set  $I'$  of rectangles: each  $R'_i$  is in contact, on all four sides, either with another rectangle of  $I'$ , or with the boundary of  $BB(\mathcal{R})$ . Note too that the sides of each  $R'_i$  lie on the grid  $\mathcal{G}$  of horizontal/vertical lines through sides of the input rectangles  $R_i$ ; the coordinates defining the rectangles  $I'$  are a subset of the set of coordinates of the input rectangles  $\mathcal{R}$ . See Figure 2.

<sup>1</sup>We consider rectangles and polygons to be closed regions that include their boundary and their interior.

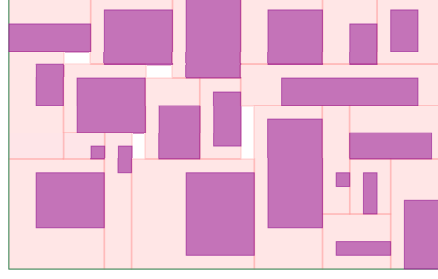


Figure 2: Example of the maximal expansions  $R'_i$  (in light red) of a set  $I$  of independent rectangles  $R_i$  (in magenta).

**The nesting relationship among maximal rectangles.** Consider a maximal rectangle,  $R'_i \in I'$ . By definition of maximality, each of the four sides of  $R'_i$  is in contact with the boundary of  $BB(\mathcal{R})$  or with the boundary of another maximal rectangle,  $R'_j$ . If  $R'_i$  and  $R'_j$  are in contact and the corresponding edge of  $R'_i$  lies within the *interior* of the corresponding edge of  $R'_j$ , then we say that  $R'_i$  is *nested* on that side where it contacts  $R'_j$ . For example, if  $R'_i$  is nested on its top side, where it contacts the bottom side of  $R'_j$ , then the left side of  $R'_j$  is strictly left of the left side of  $R'_i$ , and the right side of  $R'_j$  is strictly right of the right side of  $R'_i$ . For a rectangle  $R'_i$  that is in contact with the boundary of  $BB(\mathcal{R})$ , we say that  $R'_i$  is nested on a side that is contained in the interior of a boundary edge of the bounding box  $BB(\mathcal{R})$ . We say that  $R'_i$  is *nested vertically* if it is nested on its top side or its bottom side (or both); similarly, we say that  $R'_i$  is *nested horizontally* if it is nested on its left side or its right side (or both). Refer to Figure 4. A simple observation that comes from the definition, and the fact that rectangles in  $I'$  do not overlap, is the following:

**Observation 1.** *For a set  $I'$  of independent rectangles that are maximal within  $BB(\mathcal{R})$ , a rectangle  $R'_i \in I'$  cannot be nested both vertically and horizontally.*

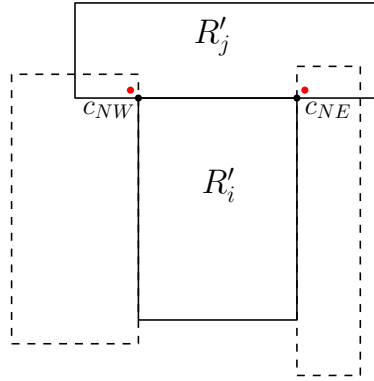


Figure 3: Proof of Observation 1: If  $R'_i$  is nested vertically, with its top side being contained in the interior of the bottom side of  $R'_j$ , then the red points, which are slightly shifted top corners of  $R'_i$ , must be interior to  $R'_j$ . If  $R'_i$  were also nested horizontally, abutting one of the dashed rectangles (of  $I'$ ) to the left/right of  $R'_i$ , then we get a contradiction to the interior disjointness of rectangles, as a red point would be interior to two rectangles of  $I'$ .

*Proof.* Consider a rectangle  $R'_i \in I'$  and assume that it is nested vertically, with its top side being a horizontal segment interior to the bottom side of a rectangle  $R'_j \in I'$  that abuts  $R'_i$  to its north. Let  $c_{NE} = (x_{max}, y_{max})$  be the northeast corner of  $R'_i$ ; then, we know from the nesting relationship with  $R'_j$ , and the assumed integrality of coordinates defining the input rectangles, that the shifted corner point

$(x_{max} + 1/2, y_{max} + 1/2)$  is interior to  $R'_j$ . Similarly, the shifted corner point  $(x_{min} - 1/2, y_{max} + 1/2)$ , just northwest of the northwest corner,  $c_{NW}$ , of  $R'_i$  is interior to  $R'_j$ . However, if  $R'_i$  were to be nested horizontally on its right side, then  $(x_{max} + 1/2, y_{max} + 1/2)$  must be interior to the abutting rectangle to the right (and a similar statement holds if  $R'_i$  were to be nested on its left side.) This is a contradiction to the interior disjointness of the rectangles of  $I'$ .  $\square$

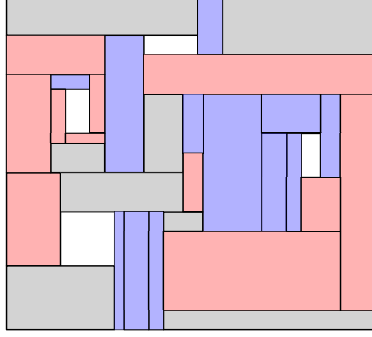


Figure 4: Example of maximal rectangles that are nested vertically (shown in blue) and nested horizontally (shown in red). Gray rectangles are not nested vertically or horizontally.

**CCR Partitions.** We define a recursive partitioning of a rectangle  $B \subseteq BB(\mathcal{R})$  as follows. At any stage of the decomposition, we have a partitioning of  $B$  into polygonal faces (*CCR faces*), each of which is a CCR. (Initially, there is a single face,  $B$ .) A set,  $\chi$ , of axis-parallel line segments (called *horizontal cut segments* and *vertical cut segments*) on the grid  $\mathcal{G}$  that partitions a CCR face  $f$  into two or more CCR faces is said to be a *CCR-cut* of  $f$ . We often use  $\sigma$  to refer to a vertical cut segment of  $\chi$ , and we will consider  $\sigma$  to be a *maximal* segment that is contained in the union of grid edges that make up  $\chi$ . A CCR-cut  $\chi$  is *K-ary* if it partitions  $f$  into at most  $K$  CCR faces. Necessarily, a *K-ary* CCR-cut  $\chi$  consists of  $O(K)$  horizontal/vertical cut segments, since each of the resulting  $K$  subfaces are (constant-complexity, orthogonal) CCR faces. In Figure 5 we show some examples of *K-ary* CCR-cuts. By recursively making *K-ary* CCR-cuts, we obtain a *K-ary* hierarchical partitioning of  $B$  into CCR faces. We refer to the resulting (finite) recursive partitioning as a *K-ary CCR-partition* of  $B$ . Associated with a CCR-partition is a *partition tree*, whose nodes correspond to the CCR faces, at each stage of the recursive partitioning, and whose edges connect a node for a face  $f$  to each of the nodes corresponding to the subfaces of  $f$  into which  $f$  is partitioned by a *K-ary* CCR-cut. The root of the tree corresponds to  $B$ ; at each level of the tree, a subset of the nodes at that level have their corresponding CCR faces partitioned by a CCR-cut, into at most  $K$  subfaces that are children of the respective nodes. The CCR faces that correspond to leaves of the partition tree are called *leaf faces*. In Figure 6 we show a CCR partition of a rectangle  $B$ , with cuts at different levels being distinguished by the color of the line segments at each level (purple, red, blue, green).

We say that a CCR-partition is *perfect* with respect to a set of rectangles if none of the rectangles have their interiors penetrated by the CCR-cuts of the CCR-partition, and each leaf face of the CCR-partition contains exactly one rectangle. (This terminology parallels the related notion of a “perfect BSP”, mentioned below.) We say that a CCR-partition is *nearly perfect* with respect to a set of rectangles if for every CCR-cut in the hierarchical partitioning each of the  $O(1)$  cut segments of the CCR-cut penetrates at most 2 rectangles of the set, and each leaf face of the CCR-partition contains at most one rectangle. (Having this property will enable a dynamic programming algorithm to optimize the size of a set of rectangles, over all nearly perfect partitions of the set, since there is only a constant amount of information to store with each subproblem defined by a CCR face in the CCR-partition.)

**Comparison with BSPs.** A binary space partition (BSP) is a recursive partitioning of a set of objects using hyperplanes (lines in 2D); a BSP is said to be *perfect* if none of the objects are cut by the hyperplanes

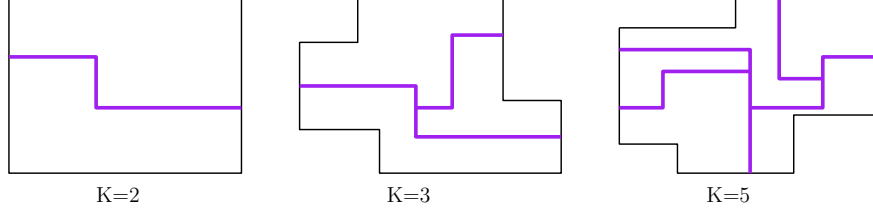


Figure 5: Examples of  $K$ -ary cuts. Left: a  $K$ -ary cut ( $K = 2$ ) of a rectangle  $B$ ; middle: a  $K$ -ary cut ( $K = 3$ ) of a CCR face; right: a  $K$ -ary cut ( $K = 5$ ) of a CCR face. Each cut consists of a set of horizontal/vertical line segments, shown in purple.

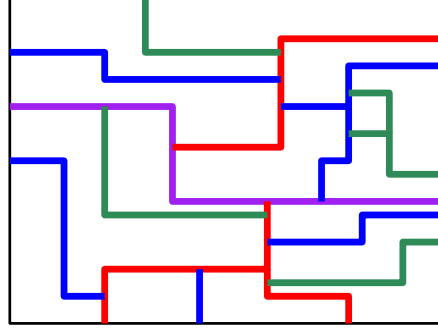


Figure 6: Example of a CCR-partition of a rectangle, with the first level cut shown in purple, the second level cuts shown in red, the third level cuts shown in blue, and the fourth level cuts shown in green. The resulting partition has 16 leaf faces.

defining the partitioning [10]. An orthogonal BSP uses cuts that are orthogonal to the coordinate axes. There are sets of axis-aligned rectangular objects for which there is no perfect orthogonal BSP; see Figure 7. A CCR-partition is a generalization of an orthogonal binary space partition (BSP), allowing more general shape faces (and cuts) in the recursive partitioning, and allowing more than 2 (but still a constant number of) children of internal nodes in the partition tree.

**Conjecture 1.** [Pach-Tardos] *For any set of  $n$  interior-disjoint axis-aligned rectangles in the plane, there exists a subset of size  $\Omega(n)$  that has a perfect orthogonal BSP.*

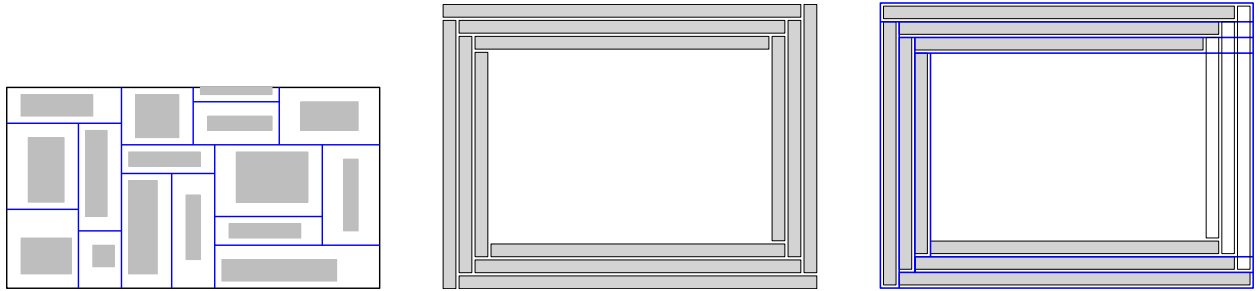


Figure 7: Left: A set of (gray) rectangles and a BSP that respects it. Middle: A set of (gray) rectangles that does not have a perfect BSP, but does have a perfect BSP of a large fraction ( $3/4$ ) subset of them. Right: A perfect CCR-partition of  $3/4$  of the rectangles in the middle figure (with  $1/4$  of the rectangles, in white, removed).

### 3 The Structure Theorem

Our main structure theorem states that for any set of  $k$  interior disjoint rectangles in the plane there is a constant fraction size subset with respect to which there exists a nearly perfect CCR-partition. We state the theorem here and we utilize it for the algorithm in the next section; the proof of the structure theorem is given in Section 5.

While Conjecture 1 remains open, and if true would imply a constant-factor approximation for MISR (via dynamic programming), our structural result suffices for obtaining a constant factor approximation (Theorem 4.1), which is based on optimizing over recursively defined CCR-partitions using dynamic programming.

**Theorem 3.1.** *For any set  $I = \{R_1, \dots, R_k\}$  of  $k$  interior disjoint (axis-aligned) rectangles in the plane within a bounding box  $B$ , there exists a  $K$ -ary CCR-partition of the bounding box  $B$ , with  $K \leq 5$ , recursively cutting  $B$  into corner-clipped rectangles (CCRs), such that the CCR-partition is nearly perfect with respect to a subset of  $I$  of size  $\Omega(k)$ .*

### 4 The Algorithm

The algorithm utilizes dynamic programming. A subproblem  $\mathcal{S}$  of the DP is specified by giving (1) a CCR  $Q$  whose edges lie on the grid  $\mathcal{G}$  defined by the set of vertical/horizontal lines through the sides of the input rectangles, and (2) a set  $I_{\mathcal{S}} \subseteq \mathcal{R}$  of  $O(1)$  input rectangles (these are “special” rectangles that we explicitly specify) that are penetrated by some of the edges of  $Q$ , at most 2 per edge. See Figure 8. Since a CCR has at most 12 edges/vertices, we know that  $|I_{\mathcal{S}}| \leq 24$  (a more careful count that exploits the structure of the cuts used in our CCR-partitions yields  $|I_{\mathcal{S}}| \leq 12$ ) and that there are only a polynomial number of possible CCRs.

For a subproblem  $\mathcal{S} = (Q, I_{\mathcal{S}})$ , let  $\mathcal{R}(\mathcal{S}) \subseteq \mathcal{R}$  denote the subset of the input rectangles that lie within  $Q$  and are pairwise disjoint from the specified rectangles  $I_{\mathcal{S}}$ . Let  $f(\mathcal{S})$  denote the cardinality of a maximum-cardinality subset,  $I^*(\mathcal{S})$ , of  $\mathcal{R}(\mathcal{S})$  that is independent and for which there exists a CCR-partition of  $Q$  that is nearly perfect with respect to  $I^*(\mathcal{S})$ .

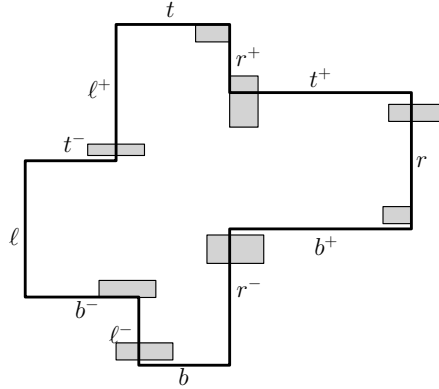


Figure 8: A subproblem  $\mathcal{S}$  defined by the CCR  $Q$  and a set  $I_{\mathcal{S}}$  of specified rectangles, with the property that at most two such rectangles are penetrated by each edge that bounds  $Q$ .

The objective for the subproblem  $\mathcal{S}$  specified by  $(Q, I_{\mathcal{S}})$  is to compute a CCR-partitioning of  $Q$  to maximize the cardinality of the subset of  $\mathcal{R}(\mathcal{S})$  with respect to which there is a CCR-partitioning of  $Q$  that is nearly perfect.

The optimization is done by iterating over all candidate  $K$ -ary ( $K \leq 5$ ) CCR-cuts of  $Q$ , together with choices of special rectangles associated with the vertical cut segments of a CCR-cut, resulting in the following

recursion:

$$f(\mathcal{S}) = \begin{cases} 0 & \text{if } \mathcal{R}(\mathcal{S}) = \emptyset, \\ \max_{\chi \in \gamma(\mathcal{S}), I_\chi} (f(\mathcal{S}_1) + \dots + f(\mathcal{S}_K) + |I_\chi|) & \text{otherwise,} \end{cases} \quad (1)$$

where the optimization is over the set,  $\gamma(\mathcal{S})$  of eligible CCR-cuts within the grid  $\mathcal{G}$  that partition  $Q$  into  $K$  CCRs ( $2 \leq K \leq 5$ ) and over the choices of the set  $I_\chi \subseteq I$  of  $O(1)$  special rectangles, with at most 2 rectangles of  $I_\chi$  penetrated by each cut segment of  $\chi$ . The cut  $\chi \in \gamma(\mathcal{S})$ , together with the choice of  $I_\chi$ , results in a set of  $K$  subproblems  $\mathcal{S}_1, \dots, \mathcal{S}_K$ , each specified by a CCR, together with a set of specified special rectangles (a subset of the  $O(1)$  rectangles of  $I_\chi$ ). Since the eligible cuts are of constant complexity within the grid of  $O(n)$  vertical/horizontal lines,  $|\gamma(\mathcal{S})|$  is of polynomial size. Also, there are a polynomial number of choices for the set  $I_\chi$ , since each set is of constant size. Thus, the algorithm runs in polynomial time.

The desired solution is given by evaluating  $f(\mathcal{S}_0)$ , on the subproblem  $\mathcal{S}_0 = (BB(\mathcal{R}), \mathcal{R})$  defined by the full bounding box,  $BB(\mathcal{R})$ , of the input set  $\mathcal{R}$  of rectangles.

The proof of correctness is based on mathematical induction on the number of input rectangles of  $\mathcal{R}$  that are contained in subproblem  $\mathcal{S}$ . The base case is determined by subproblems  $\mathcal{S}$  for which there is no rectangle of  $\mathcal{R}$  inside the CCR; we correctly set  $f(\mathcal{S}) = 0$  for such subproblems. With the induction hypothesis that  $f(\mathcal{S})$  is correctly computed for subproblems  $\mathcal{S}$  containing at most  $k$  rectangles of  $\mathcal{R}$ , we see that, for a subproblem  $\mathcal{S}$  having  $k + 1$  rectangles of  $\mathcal{R}$ , since we optimize over all CCR-cuts partitioning  $Q$  into at most 5 CCRs, respecting  $I_\mathcal{S}$ , and over all choices of  $O(1)$  special rectangles penetrated by each considered CCR-cut, with each of the values  $f(\mathcal{S}_i)$  being correctly computed (by the induction hypothesis), we obtain a correct value  $f(\mathcal{S})$ . Since the algorithm runs in polynomial time, and our structure theorem shows that there exists an independent subset of  $\mathcal{R}$  of size at least  $\Omega(k^*)$  for which there is a CCR-partition respecting this subset, we obtain our main result:

**Theorem 4.1.** *There is a polynomial-time  $O(1)$ -approximation algorithm for maximum independent set for a set of axis-aligned rectangles in the plane.*

*Remark.* While efficiency is not the focus of our attention here, other than to establish polynomial-time, we comment briefly on the overall running time of the dynamic program. A naive upper bound comes from the fact that there are at most  $O(n^{12})$  CCRs defined on the set of vertical/horizontal lines through sides of the input rectangles, and there are at most  $O(n^{12})$  specified rectangles  $I_\mathcal{S}$  in any subproblem. The most complex cut  $\chi$  among all of the cases is seen to be (in case (3)(c)) a cut having 6 horizontal cut segments and 2 vertical cut segments, each having at most 2 associated specified rectangles; thus, there are at most  $O(n^{10})$  choices for  $(\chi, I_\chi)$ . Thus, the optimization is over at most  $O(n^{10})$  choices, for each of at most  $O(n^{24})$  subproblems. The overall time bound of  $O(n^{34})$  is surely an over-estimate.

## 5 Proof of the Structure Theorem

*Proof.* In this section we prove the main structure theorem, Theorem 3.1, which stated that for any set  $I = \{R_1, \dots, R_k\}$  of  $k$  interior disjoint (axis-aligned) rectangles in the plane within a bounding box  $B$ , there exists a  $K$ -ary CCR-partition of the bounding box  $B$ , with  $K \leq 5$ , recursively cutting  $B$  into corner-clipped rectangles (CCRs), such that the CCR-partition is nearly perfect with respect to a subset of  $I$  of size  $\Omega(k)$  (at least  $k/4$ , though, later, we describe how the factor 4 improves to factor 3).

First, we consider the set  $I'$  of maximal expansions, as described previously, of the  $k$  input rectangles  $I = \{R_1, \dots, R_k\}$  within  $B$ . Recall that, appealing to Observation 1, the set  $I'$  is the disjoint union of subsets:  $I' = I_h \cup I_v \cup I_0$ , where  $I_h$  is the subset of “red” rectangles that are nested horizontally,  $I_v$  is the subset of “blue” rectangles that are nested vertically, and  $I_0$  is the subset of “gray” rectangles that are not nested on any of their four sides. Refer to Figure 4. It cannot be that both  $|I_h|$  and  $|I_v|$  are greater than  $k/2$ ; thus, assume, without loss of generality, that  $|I_h| \leq k/2$ . Then, there are  $|I_v| + |I_0| \geq k/2$  “non-red” rectangles.<sup>2</sup>

---

<sup>2</sup>Throughout the discussion going forward in this section, the assumption that the number of red (maximal) rectangles



We now describe a process by which a subset of  $\Omega(k)$  of the rectangles of  $I'$  is chosen, and a CCR-partition,  $\Pi$ , is constructed that is nearly perfect with respect to this subset, and, thus, by the following claim, is nearly perfect with respect to the corresponding subset of (sub-)rectangles  $I$ .

**Claim 5.1.** *If a CCR-partition is nearly perfect with respect to a set  $A' \subset I'$  of maximal rectangles, then it is nearly perfect with respect to the corresponding set  $A \subseteq I$  of input rectangles.*

*Proof.* This follows immediately from the fact that, for each  $R' \in I'$ , the corresponding  $R \in I$  is a subrectangle of  $R'$ .  $\square$

Initially, all rectangles of  $I'$  are *active*. During the process of recursively partitioning  $BB(\mathcal{R})$  into a CCR-partition, a subset of the rectangles of  $I'$  will be discarded and removed from active status. In the end, the set of remaining active rectangles of  $I'$  have the property that the CCR-partition is nearly perfect with respect to the remaining active rectangles. We show (Claim 5.9), via a charging scheme, that at most a constant fraction ( $3/4$ ) of the rectangles of  $I'$  are discarded, implying that the final set of active rectangles of  $I'$  has cardinality at least  $k/4 = |I'|/4$ . (At the end of this section we describe how the factor 4 is improved to a factor 3, with a slight modification.)

At each stage in the recursive partitioning, a CCR  $Q$  that contains more than one rectangle of  $I'$  (and thus more than one rectangle of  $I$ ) is partitioned via a cut  $\chi$ , within the grid  $\mathcal{G}$ , into at most  $K = 5$  CCR faces, via a set of  $O(1)$  horizontal and vertical cut segments. Details of how we determine these CCR-cuts are presented in the statement and proof of Lemma 5.2, below, after we introduce the notion of “fences”.

A property of the cuts  $\chi$  we construct is that no rectangle of  $I'$  is crossed by a horizontal cut segment (Lemma 5.2, (iii), together with the property that the horizontal segments (“fences”) that serve as input to the lemma are defined to have the property that they do not cross any of the rectangles of  $I'$ ); horizontal cut segments can follow the boundary of a rectangle of  $I'$ , and might penetrate up to two rectangles of  $I'$  (one at each end of the segment), but cannot cross any such rectangle.

A vertical cut segment,  $\sigma$ , of  $\chi$  can penetrate and also cross some rectangles of  $I'$ , and we discard those rectangles that are *crossed* by such a cut segment  $\sigma$ . (On any vertical cut segment at most two rectangles (the first and last, at each end of the segment) can be *penetrated* but not *crossed*; these rectangles will not be discarded and are the source of the use of “nearly perfect” cuts in our method.) The ability to find such cuts  $\chi$  is assured by Lemma 5.2. Those rectangles that are crossed by a vertical cut segment and discarded must be accounted for, to assure that a significant fraction remain in the end. This is where a charging scheme is utilized, which we describe below, after we introduce fences.

**Fences.** An important aspect of the method we will describe for construction of a CCR-partition that respects a large subset of  $I'$  is the enforcement of constraints that prevent the cuts we produce from crossing rectangles without being able to “pay” for the crossing, through our charging scheme (below). We achieve this by erecting certain *fences*, which are horizontal line segments, on the grid  $\mathcal{G}$ , each “anchored” on a left/right side of the current CCR face,  $Q$ . The fences become constraints on CCR-cuts of  $Q$ , as we require that a CCR-cut  $\chi$  have no vertical cut segments that cross any fence (and all horizontal cut segments will be contained within the set of fence segments); refer to Lemma 5.2 below.

For each of the 4 corners,  $c_{NE}$ ,  $c_{NW}$ ,  $c_{SW}$ ,  $c_{SE}$ , of a rectangle  $R \in I'$ , we let the corresponding *shifted* corner (denoted  $c'_{NE}$ ,  $c'_{NW}$ ,  $c'_{SW}$ ,  $c'_{SE}$ ) be the point interior to  $R$ , shifted towards the interior of  $R$  by  $1/2$  in both  $x$ - and  $y$ -coordinates (recall that the defining coordinates of the input rectangles are assumed, without loss of generality, to be integers); for example, if  $c_{NE} = (x, y)$ , then  $c'_{NE} = (x - 1/2, y - 1/2)$ . (There is nothing special about the number  $1/2$ ; any real number strictly between 0 and 1 could be used to define shifted corners for the rectangles, which have integer coordinates.) We focus attention on northeast and northwest corners, as our charging scheme will be described in terms of them.

---

is at most  $k/2$  will permeate, leading to apparent “bias” in places where we construct “fence” segments that are horizontal, require constraints on vertical cut segments in Lemma 5.2, focus on charging off rectangles that are crossed by vertical cut segments, while horizontal cut segments never cross rectangles of  $I'$ , etc; in all of these places, there is a symmetric statement corresponding to the case in which, instead, the number of blue (maximal) rectangles is at most  $k/2$ , and there are at least  $k/2$  “non-blue” rectangles.

We say that the northeast corner,  $c$ , of a rectangle  $R \in I'$ , is *exposed to the right within  $Q$*  if a horizontal rightwards ray,  $\rho$ , with endpoint at its corresponding shifted corner,  $c'$ , does not penetrate any rectangle of  $I'$  (other than  $R$ ) that lies fully within  $Q$  before reaching the right boundary of  $Q$  (segments  $r$ ,  $r^+$ , or  $r^-$ ). If the northeast corner,  $c$ , of rectangle  $R$  is *not* exposed to the right within  $Q$ , then the rightwards ray  $\rho$  penetrates at least one rectangle that lies fully within  $Q$  before reaching the right boundary of  $Q$ ; the first such rectangle,  $R'$ , that is penetrated by  $\rho$  after  $\rho$  exits  $R$  is called the *right-neighbor* of  $R$ . We similarly define the notion of a northwest corner being exposed to the left within  $Q$  and the notion of a left-neighbor of  $R$  (in the case that the corner is not exposed to the left). Note that, from the definition, the northeast corner of  $R$  is exposed to the right (resp., left) if and only if the northwest corner of  $R$  is exposed to the right (resp., left). Thus, we say that the top side of  $R$  is exposed to the left (resp., right) if the northeast and northwest corners of  $R$  are exposed to the left (resp., right).

When a CCR  $Q$  is partitioned by a CCR-cut,  $\chi$ , a vertical cut segment,  $\sigma$ , of  $\chi$  may cause some top sides of other rectangles of  $I'$  within the new CCR faces (subfaces of  $Q$  on either side of  $\sigma$ ) to become exposed to the left or to the right within their respective new CCR faces. When a vertical cut segment  $\sigma$  of a CCR-cut causes the top side of  $R$  to become exposed to its left (resp., right) within its new CCR face, we establish a fence (horizontal line segment) that includes the top side of  $R$  and extends to the left (resp., right) boundary of the CCR face (at a point on  $\sigma$  that gave rise to the new exposure) and extends to the right (resp., left) side of the right-neighbor (resp., left-neighbor) of  $R$ .<sup>3</sup> Note that, by its definition, a fence segment does not cross any rectangle of  $I'$ ; it may penetrate a rectangle of  $I'$  on its left end and/or its right end (and may cross the input rectangle that is contained within a penetrated maximal rectangle of  $I'$ ). Refer to Figure 9; we use the convention that fences are shown in red (resp., blue) if anchored on their left (resp., right) endpoint. (This color choice of red/blue for fences has nothing to do with the “red” and “blue” color terminology we had above for rectangles in the set  $I_h$  and  $I_v$ .) We establish fences with each cut in order to maintain the following invariant during the course of the recursive partitioning:

[Fence Invariant] *For each rectangle  $R \in I'$  that lies fully within a CCR  $Q$ , if the top side of  $R$  is exposed to the left (resp., right) within  $Q$ , then there is a (horizontal) fence segment  $\alpha$  (resp.,  $\beta$ ) that includes the top side of  $R$  and extends leftwards to the left side of  $Q$  and rightwards to the right side of the right-neighbor of  $R$  (resp., extends rightwards to the right side of  $Q$  and leftwards to the left side of the left-neighbor of  $R$ ).*

*If a rectangle  $R \in I'$  is crossed by a vertical cut segment  $\sigma$ , then there is a (horizontal) fence segment  $\alpha$  established that extends the top side of  $R$  leftwards from  $\sigma$  to the left side of the left-neighbor of  $R$  and a (horizontal) fence segment  $\beta$  established that extends the top side of  $R$  rightwards from  $\sigma$  to the right side of the right-neighbor of  $R$ .*

We say that a rectangle  $R \in I'$ , with  $R$  contained within a CCR  $Q$ , is *anchored* if its top side is contained within the top boundary of  $Q$  or within a fence segment within  $Q$ , anchored on the left or the right of  $Q$ . Lemma 5.2 guarantees that the CCR-cuts we utilize do not have any vertical cut segments  $\sigma$  that cross any fences and, therefore, do not cross any anchored rectangles (since a vertical segment that crosses a rectangle necessarily crosses its top and bottom sides). It can be, however, that a vertical cut segment  $\sigma$  penetrates (without crossing) an anchored rectangle, e.g., if the segment  $\sigma$  terminates on a fence or on a top/bottom side of  $Q$ ; however, a vertical cut segment  $\sigma$  can penetrate, without crossing, at most two anchored rectangles, one incident to the top endpoint and one incident to the bottom endpoint of  $\sigma$ . (This is the source of the “2” in the definition of a nearly perfect cut.) Each rectangle  $R \in I'$  is a maximal expansion of an original input rectangle of  $I$ ; since the original rectangle is a subrectangle of  $R$ , it can happen that a vertical cut segment  $\sigma$  crosses the original rectangle (or it could completely miss intersecting it) associated with an anchored rectangle  $R \in I'$ , while not *crossing*, but only *penetrating*,  $R$ .

<sup>3</sup>In an earlier version of this paper [19], the fence segment extended only to the right (or left) side of the rectangle  $R$ , rather than continuing to the right (or left) side of the right-neighbor (or left-neighbor) of  $R$ . By extending the fence through the neighbor, we are able to refine the charging analysis, so that each rectangle that is charged is charged from only one side, rather than from both sides, as the extended fence ensures that the neighbor is not crossed by a cut, which might lead to  $R$  being charged from its other side.

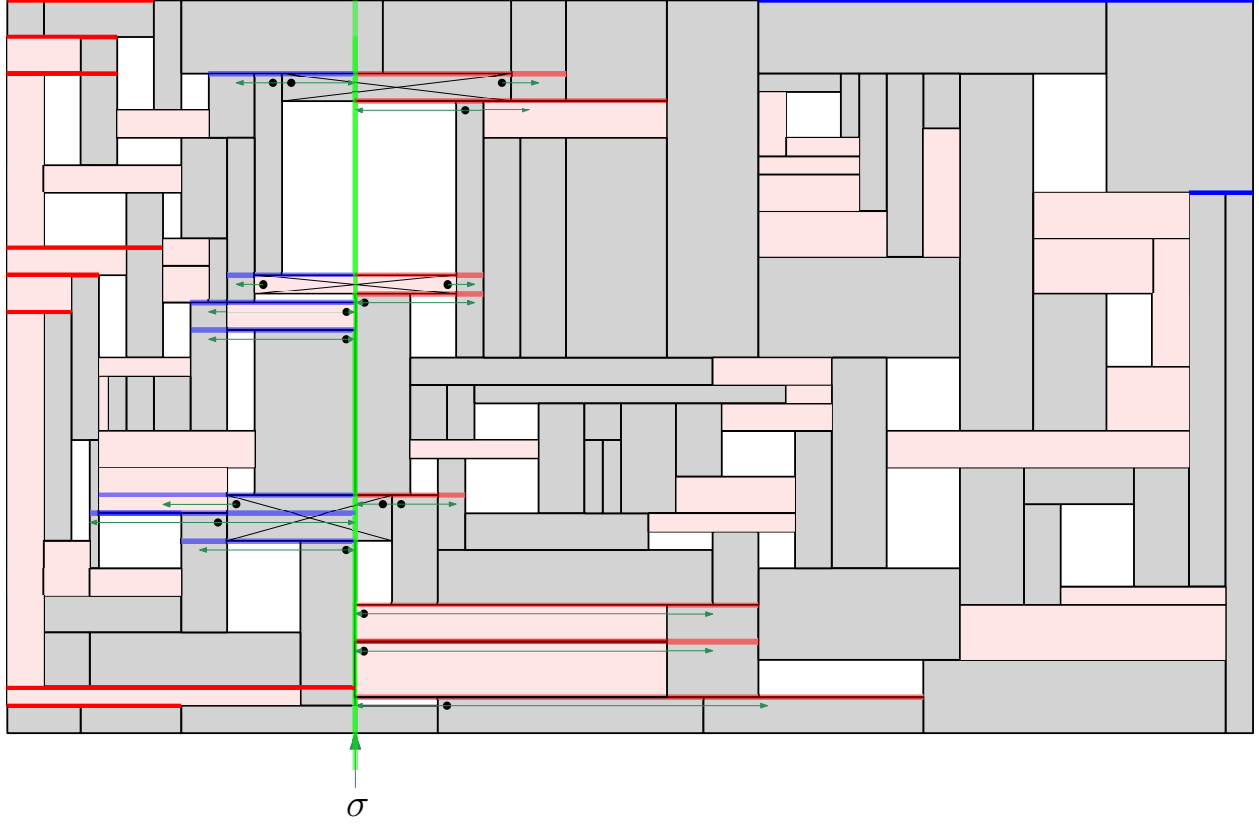


Figure 9: Example showing the establishment of fences after a cut. In this figure, the CCR is a rectangle, the maximal rectangles are shown, with red ones (nested to the left or to the right) shown in light red, and all non-red rectangles shown in gray. A vertical cut segment  $\sigma$  (in green) is shown. The cut results in the top sides of some rectangles becoming exposed; we show the respective shifted corners as black solid dots, with dark green arrows showing the exposure to the cut  $\sigma$ , as well as showing the additional penetrated abutting rectangle, which defines the extent of the fence segment. Rectangles that are *crossed* by the cut are marked with an “X”: By the Fence Invariant, when a rectangle is crossed by a vertical cut segment, we establish a fence segment extending leftwards through the left-neighbor of  $R$  and rightwards through the right-neighbor of  $R$ . (Note that the first and last rectangles intersected by  $\sigma$  are penetrated but not crossed by  $\sigma$ .) All of the newly established fences, anchored on  $\sigma$ , are shown in red (if the left endpoint is anchored on  $\sigma$ ) or in blue (if the right endpoint is anchored on  $\sigma$ ).

Lemma 5.2 below shows that the recursive partitioning process is feasible, showing that for any CCR face  $Q$  and any set of (horizontal) fences anchored on the left/right sides of  $Q$ , it is always possible to find a CCR-cut with the properties claimed in the lemma; in particular, the cut should “respect” the given set of fences, in that no vertical cut segment of the cut crosses a fence segment. We initialize the set of fences in order that the Fence Invariant holds at the beginning of the process: for each rectangle  $R \in I'$  whose top side is exposed to the left within  $B$ , we establish a fence along its top side, anchored on the left side of  $B$ , extending rightwards to the right side of the right-neighbor of  $R$ . (If the top side of  $R$  is contained within the top side of  $B$ , we need not establish a fence, since the fence segment would be contained in the top side of  $B$ .) We do similarly for rectangles whose top side is exposed to the right within  $B$ . See Figure 10. If there exists a rectangle  $R \in I'$  whose top side is exposed both to the left and to the right within  $B$ , then we simply cut  $B$  with a horizontal cut segment along the top side of  $R$ , from the left side of  $B$  to the right side of  $B$ , since this horizontal segment penetrates no rectangles of  $I'$ .

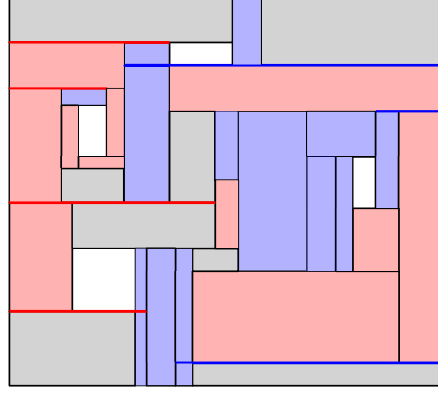


Figure 10: The initial fences, shown as bold red/blue segments, for the shown set of maximal rectangles within a rectangle  $B$ .

We appeal to the following key technical lemma, whose proof is based on a careful enumeration of cases, detailed in the appendix.

**Lemma 5.2.** *Let  $I'$  be a set of maximal rectangles associated with an independent set  $I$  of rectangles. Let  $Q$  be a CCR whose edges lie on the grid lines of  $\mathcal{G}$ , defined by the coordinates of the rectangles  $I'$  (and thus of  $I$ ). Let  $\{\alpha_1, \dots, \alpha_{k_\alpha}\}$  be a set of “red” horizontal anchored (grid) segments within  $Q$ , that are anchored with left endpoints on the left sides ( $\ell$ ,  $\ell^+$ , or  $\ell^-$ ) of  $Q$ , and let  $\{\beta_1, \dots, \beta_{k_\beta}\}$  be a set of “blue” horizontal anchored (grid) segments within  $Q$ , that are anchored with right endpoints on the right sides ( $r$ ,  $r^+$ , or  $r^-$ ) of  $Q$ . Then, assuming that  $Q$  contains at least two grid cells (faces of  $\mathcal{G}$ ), there exists a CCR-cut  $\chi$  with the following properties:*

- (i)  $\chi$  partitions  $Q$  into  $O(1)$  (at most 5) CCR faces;
- (ii)  $\chi$  is comprised of  $O(1)$  horizontal/vertical segments on the grid  $\mathcal{G}$ , with endpoints on the grid;
- (iii) horizontal cut segments of  $\chi$  are a subset of the given red/blue anchored segments;
- (iv) vertical cut segments of  $\chi$  do not cross any of the given red/blue anchored segments;
- (v) there are at most 2 vertical cut segments of  $\chi$ .

The lemma shows that a CCR,  $Q$ , with anchored (grid) segments has a CCR-cut, on the grid, partitioning  $Q$  into at most 5 CCRs (CCR faces in the grid). Applying this recursively (and finitely, due to the finiteness of the grid), until there is at most one rectangle of  $I'$  interior to each CCR face, we will be able to conclude, based on the charging scheme below, the proof of the claimed structure theorem.

*Remark.* There is an equivalent “rotated” version of Lemma 5.2 that applies to a set of vertical (fence) segments anchored on the top/bottom sides of  $Q$ , with vertical cut segments lying along the anchored segments, and (at most 2) horizontal cut segments not crossing any anchored (vertical) segments. The rotated version applies in our proof of the structure theorem in the case that the non-blue maximal rectangles have cardinality at least  $k/2$ .

**Charging Scheme.** Consider a vertical cut segment,  $\sigma$ , that is part of a CCR-cut  $\chi$  of a CCR  $Q$ , given by Lemma 5.2. The segment  $\sigma$  penetrates some (possibly empty) subset,  $I'_\sigma$ , of rectangles of  $I'$  that lie within  $Q$ ; the intersection of  $\sigma$  with the rectangles  $I'_\sigma$  is a set of subsegments of  $\sigma$ , at most two of which are *not* contained within the interior of  $\sigma$ . (For a subsegment of  $\sigma$  not to be interior to  $\sigma$ , the subsegment must share an endpoint with  $\sigma$ .) Thus, at most two of the rectangles of  $I'_\sigma$  are not *crossed* by  $\sigma$ .

**Claim 5.3.** *None of the rectangles of  $I'_\sigma$  that are crossed by  $\sigma$  have a top side that is exposed to the left or right within  $Q$ .*

*Proof.* This is immediate from the Fence Invariant, and the fact (Lemma 5.2, part (iv)) that vertical cut segments do not cross fences.  $\square$

Our charging scheme assigns (“charges off”) each *non-red* rectangle  $R$  that is crossed by a vertical cut segment  $\sigma$  to a corner (northwest or northeast) of a rectangle of  $I'$ . If the rectangle  $R$  is *red*, we do not attempt to charge it off, as our charging scheme is based on charging to corners of rectangles that lie to the left/right of  $R$  (within the vertical extent of  $R$ ), and a red rectangle is, by definition, nesting on its left or on its right (or both), implying that we will not have available the corners we need to be able to charge. Instead, our accounting scheme below will take advantage of the fact that the number of non-red rectangles is at least  $k/2$ .

Consider a non-red rectangle  $R \in I'$  within  $Q$  that is crossed by a vertical cut segment  $\sigma$ . By property (v) of Lemma 5.2, it must be the case that either there is no vertical cut segment of  $\chi$  to the right of  $\sigma$  or there is no vertical cut segment of  $\chi$  to the left of  $\sigma$ . Assume, without loss of generality, that there is no vertical cut segment to the right of  $\sigma$ . Then, we charge the crossing of  $R$  to a northwest corner of a rectangle of  $I'$  that lies to the right of  $R$ . (If, instead, there is no vertical cut segment to the left of  $\sigma$ , then we charge  $R$  to a northeast corner of some rectangle of  $I'$  that lies to the left of  $R$ .) Specifically, let  $c$  be the northeast corner of  $R$ , and let  $c'$  be the corresponding shifted corner (slightly to the southwest of  $c$ ). By Claim 5.3,  $c$  is not exposed to the right within  $Q$ ; thus, the rightwards horizontal ray from  $c'$  must penetrate at least one rectangle of  $I'$  within  $Q$  before reaching the right boundary of  $Q$ . Let  $R_r$  be the first (leftmost) rectangle that is penetrated. Let  $y^+$  and  $y^-$  (resp.,  $y_r^+$  and  $y_r^-$ ) be the top and bottom  $y$ -coordinates of rectangle  $R$  (resp.,  $R_r$ ). Similarly, let  $x^+$ ,  $x^-$ ,  $x_r^+$ , and  $x_r^-$  denote the  $x$ -coordinates of the left/right sides of  $R$  and  $R_r$ , so that  $R = [x^-, x^+] \times [y^-, y^+]$  and  $R_r = [x_r^-, x_r^+] \times [y_r^-, y_r^+]$ . By definition of  $R_r$ , we know that  $y_r^+ \geq y^+$  and that  $x^+ \leq x_r^-$ . Refer to Figure 11, where we illustrate the charging scheme, enumerating the 8 potential cases, depending if (i)  $y^+ = y_r^+$  or  $y^+ < y_r^+$ , (ii)  $y^- > y_r^-$  or  $y^- \leq y_r^-$ , (iii)  $x^+ = x_r^-$  or  $x^+ < x_r^-$ . We itemize the 8 cases below:

- (1) [ $y^+ = y_r^+$ ,  $y^- > y_r^-$ , and  $x^+ = x_r^-$ .] We charge the northwest corner,  $c_r$ , of rectangle  $R_r$ .

After the cut along  $\sigma$ , rectangle  $R_r$  will have its top side exposed to the left, so, to maintain the Fence Invariant, we establish a horizontal fence segment (shown in red), which includes the top side of  $R_r$ , and extends rightwards to the right side of the right-neighbor,  $R'_r$ , or  $R$ . (We know that the top side of  $R_r$  is not exposed to the right side of  $Q$ , since, if it were exposed, then, by the Fence Invariant, there would be a fence extending along the top side of  $R_r$ , and leftwards through  $R$  (the left-neighbor of  $R_r$ ), to the left side of  $R$ , implying that  $\sigma$  crosses a fence, a contradiction.) This fence will become exposed to the left (at a point along  $\sigma$ ) after the cut along  $\sigma$ . In the figure, we show  $R'_r$  abutting  $R_r$ , but this need not be the case.

- (2) [ $y^+ = y_r^+$ ,  $y^- > y_r^-$ , and  $x^+ < x_r^-$ .] In this case, there is a rectangular region (shown in gray in the figure) separating the right side of  $R$  from the left side of  $R_r$ . This gray rectangle must intersect the interior of at least one rectangle of  $I'$ ; otherwise,  $R$  is not maximal, as it can be extended to the right, until it abuts  $R_r$ . Thus, there must be some rectangle in  $I'$  whose interior overlaps with the interior of the gray rectangle; let  $W \in I'$  be such a rectangle whose top side has the maximum  $y$ -coordinate among all such rectangles. Then, we get a contradiction as follows: If the top side of  $W$  lies at or above the top sides of  $R$  and  $R_r$ , then the rightwards ray from  $c'$  penetrates  $W$  before penetrating  $R_r$ , contradicting the definition of  $R_r$ ; on the other hand, if the top side of  $W$  lies below the rightwards ray from  $c'$ , then we get a contradiction to the maximality of  $W$ , since it can be extended upwards, to the top of the gray rectangle. Thus, this case cannot happen.

- (3) [ $y^+ = y_r^+$ ,  $y^- \leq y_r^-$ , and  $x^+ = x_r^-$ .] This is handled exactly as in case (1): we charge the northwest corner  $c_r$  and establish the fence segment (shown in red), through the top side of  $R_r$ , extending to the right side of  $R'_r$ .

- (4) [ $y^+ = y_r^+$ ,  $y^- \leq y_r^-$ , and  $x^+ < x_r^-$ .] Exactly as in case (2), this case cannot happen.

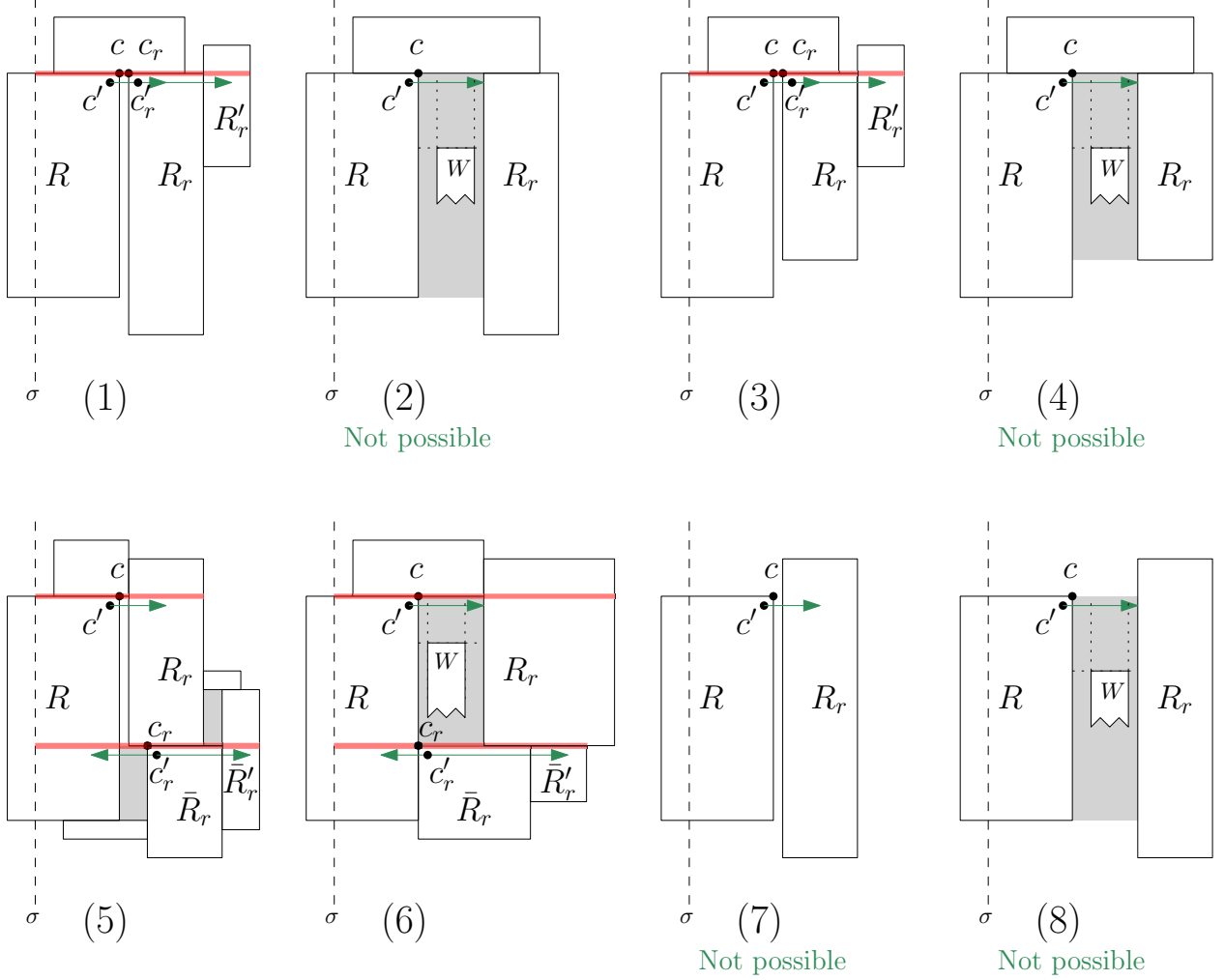


Figure 11: Case analysis for the charging scheme when a non-red rectangle  $R$  is crossed by a vertical portion (shown dashed),  $\sigma$ , of a cut  $\chi$ . The charged corner is labelled  $c_r$ , for the possible cases (1), (3), (5), (6). The fences established after the cut are shown in red. Here, we only show the case of charging to the right of the crossed rectangle  $R$ .

- (5)  $[y^+ < y_r^+, y^- \leq y_r^-, \text{ and } x^+ = x_r^-]$  By maximality, there must be at least one rectangle abutting  $R_r$  from below, whose top side overlaps with the bottom side of  $R_r$ . Let  $\bar{R}_r$  be such an abutting rectangle with leftmost left side; then,  $R$  must be the left-neighbor of  $\bar{R}_r$ , implying that the top side of  $\bar{R}_r$  is not exposed to the right, since, by the Fence Invariant, this would imply that a fence exists along the top side of  $\bar{R}_r$ , extending leftwards through  $R$  (the left-neighbor of  $\bar{R}_r$ ), contradicting the fact that  $\sigma$  does not cross any fence. (Note that  $\bar{R}_r$  may or may not be abutting  $R$ .) We charge the northwest corner,  $c_r$ , of rectangle  $\bar{R}_r$ .

After the cut along  $\sigma$ , rectangle  $\bar{R}_r$  will have its top side exposed to the left, so, to maintain the Fence Invariant, we establish a horizontal fence segment (shown in red), which includes the top side of  $\bar{R}_r$ , extending leftwards to  $\sigma$  and extending rightwards to the right side of the right-neighbor,  $\bar{R}'_r$ , of  $\bar{R}_r$ . Maintenance of the Fence Invariant also implies that we establish a fence along the top side of  $R$ , extending rightwards to the right side of  $R_r$ , the right-neighbor of  $R$ .

- (6)  $[y^+ < y_r^+, y^- \leq y_r^-, \text{ and } x^+ < x_r^-]$  By maximality, there must be at least one rectangle abutting  $R_r$  whose top side overlaps with the bottom edge of  $R_r$ ; let  $\bar{R}_r$  be such an abutting rectangle with leftmost left side. We charge the northwest corner,  $c_r$ , of rectangle  $\bar{R}_r$ .

Consider the gray rectangle,  $[x^+, x_r^-] \times [y_r^-, y^+]$ . First, note that there can be no rectangle in  $I'$  whose interior overlaps with this gray rectangle, for, if such a rectangle existed, then there exists such a rectangle with a maximum  $y$ -coordinate of its top side, and such a rectangle fails to be maximal (since the rightwards ray from  $c'$  first penetrates  $R_r$  after it exits  $R$ ). We claim that  $R$  is the left-neighbor of  $\bar{R}_r$ . Otherwise, there is a rectangle,  $W$ , that is penetrated by the leftwards ray from  $c'_r$  before it enters  $R$ , implying that the top side of  $W$  has  $y$ -coordinate at least  $y_r^-$ , which implies that  $W$  is not maximal. ( $W$  cannot have its top side abutting  $R_r$ , since we chose  $\bar{R}_r$  to have leftmost left side among such rectangles abutting  $R_r$ .) Thus, after the cut along  $\sigma$ , rectangle  $\bar{R}_r$  will have its top side exposed to the left. In order to maintain the Fence Invariant, we establish a horizontal fence segment (shown in red), which includes the top side of  $\bar{R}_r$ , extends leftwards to  $\sigma$ , and extends rightwards to the right side of the right-neighbor,  $\bar{R}'_r$ , of  $\bar{R}_r$ . (We know that there must be a right-neighbor, since, if the top side of  $\bar{R}_r$  were exposed, then, by the Fence Invariant, there would be a fence extending along the top side of  $\bar{R}_r$ , and leftwards through  $R$  (the left-neighbor of  $\bar{R}_r$ ), to the left side of  $R$ , implying that  $\sigma$  crosses a fence, a contradiction.) Maintainance of the Fence Invariant also implies that we establish a fence along the top side of  $R$ , extending rightwards to the right side of  $R_r$ , the right-neighbor of  $R$ .

- (7)  $[y^+ < y_r^+, y^- > y_r^-, \text{ and } x^+ = x_r^-]$  We get a contradiction to the fact that  $R$  is non-red, since the inequalities  $y^+ < y_r^+$  and  $y^- > y_r^-$  say that  $R$  is nesting on its right. Thus, this case cannot happen.
- (8)  $[y^+ < y_r^+, y^- > y_r^-, \text{ and } x^+ < x_r^-]$  By reasoning exactly as in case (2), this case cannot happen.

Summarizing the above case enumeration of the charging scheme, we state the following facts:

**Claim 5.4.** *If the northwest corner of a rectangle is charged for the crossing of  $R$ , then  $R$  is the left-neighbor of the rectangle whose corner is charged. (A symmetric statement holds when a northeast corner is charged.)*

*Proof.* This fact is immediate from the specification of the charged corner. (Refer to Figure 11.)

Specifically, in cases (1) and (3), when we charge the northwest corner,  $c_r$ , of rectangle  $R_r$ , the leftwards ray from  $c'_r$  penetrates  $R$  immediately after it exits  $R_r$ , so  $R$  is, by definition, the left-neighbor of  $R_r$ .

In case (5), when we charge the northwest corner,  $c_r$ , of rectangle  $\bar{R}_r$ , the leftwards ray from  $c'_r$  must penetrate  $R$  before penetrating any other rectangle of  $I'$ : If it instead penetrated some other rectangle  $R''$ , then the top side of  $R''$  must be overlapping the bottom side of  $R_r$ , and  $R''$  would then be a rectangle abutting  $R_r$ , with left side to the left of the left side of  $\bar{R}_r$ , contradicting the choice of  $\bar{R}_r$  having the leftmost left side among abutting rectangles. Thus,  $R$  is the left-neighbor of  $\bar{R}_r$  in case (5).

In case (6), when we charge the northwest corner,  $c_r$ , of rectangle  $\bar{R}_r$ , the leftwards ray from  $c'_r$  must penetrate  $R$  before penetrating any other rectangle of  $I'$ , since we argued in case (6) that the left side of  $\bar{R}_r$  must overlap the right side of  $R$ , which is abutting  $\bar{R}_r$  to its left. Thus,  $R$  is the left-neighbor of  $\bar{R}_r$  in case (6).  $\square$

**Claim 5.5.** *A corner of a rectangle is charged at most once.*

*Proof.* This is an immediate consequence of Claim 5.4, since there is a unique left-neighbor,  $R$ , of the rectangle whose corner is charged. (Also, once a corner is charged, a fence is established that prevents any vertical cut segment that would ever expose (again) the corner to the left.)  $\square$

**Claim 5.6.** *If a northwest corner,  $c_r$ , of rectangle  $R_r \in I'$  is charged, then  $R_r$  has not previously been crossed by a vertical cut segment, is not currently (as part of  $\chi$ ) crossed by a vertical cut segment, and will not be crossed by vertical cut segments later in the recursive CCR-partition.*

*Proof.* If  $R_r$  had previously been crossed by a vertical cut segment,  $\sigma'$ , then the corner  $c$  of  $R$  would have become exposed to the right, and a fence segment would have been established through  $c$  and the top side of  $R$  (extending leftwards to the left side of the left-neighbor of  $R$ ); this fence prevents  $R$  from being crossed, since a vertical cut segment never crosses a fence segment.

No other vertical cut segment of  $\chi$  currently lies to the right of  $\sigma$  (recall property (v) of Lemma 5.2, and the assumption, without loss of generality, that it is the right side of  $\sigma$  that has no vertical cut segment of  $\chi$ ); thus,  $R_r$  is not crossed by a vertical cut segment of  $\chi$ . (In the modification described below that results in an improved approximation factor, we enable charging to *both* sides, left and right, of a crossed rectangle  $R$ , using “two-stage” cuts when there are two vertical cut segments in the cut given by Lemma 5.2.)

Later in the recursive CCR-partition, the rectangle  $R_r$  cannot be crossed by a vertical cut segment, since such a crossing would imply a crossing of the fence we established through the top side of  $R_r$  (and this is ruled out by property (iv) of Lemma 5.2. Indeed, we establish fences in order to enforce that once a rectangle has a corner charged, it cannot be crossed by later cuts in the recursive partitioning.  $\square$

**Claim 5.7.** *At most one corner of a rectangle is charged: either the northwest corner or the northeast corner.*

*Proof.* By Claim 5.4, if the northwest corner of a rectangle  $R' \in I'$  is charged for the crossing of a rectangle  $R$ , then  $R$  is the left-neighbor of the rectangle  $R'$ ; further, by the Fence Invariant, a fence is established along the top side of  $R'$ , extending rightwards to the right side of the right-neighbor of  $R'$ . This fence prevents the right-neighbor of  $R'$  from being crossed by a vertical cut segment; thus, the northeast corner of  $R'$  cannot be charged, since, by Claim 5.4, if the northeast corner were charged for the crossing of some rectangle  $R''$ , then  $R''$  must be the right-neighbor of  $R'$ , and we know that the right-neighbor of  $R'$  cannot be crossed by a vertical cut segment, since it is protected by the previously established fence.  $\square$

The set of red rectangles can be partitioned into two sets: those that are cut (let  $h_\chi$  be the number) and those that are not cut (let  $h_0$  be the number). Similarly, non-red rectangles can be partitioned into two sets: those that are cut (let  $m_\chi$  be the number) and those that are not cut (let  $m_0$  be the number). By Claim 5.6, if any rectangle is charged, then it is never crossed by a cut; thus, there are at most  $h_0 + m_0$  rectangles that are charged, and we know from Claim 5.5 that the amount of charge received by any of these rectangles is at most 1 (one unit of charge on one corner, northwest or northeast). We conclude that

**Claim 5.8.** *The total sum of all charges is at most  $h_0 + m_0$ , and thus  $m_\chi \leq h_0 + m_0$ .*

*Proof.* By Claim 5.7, at most 1 corner of a rectangle is charged, and by Claim 5.5, each is charged at most once. Since, by specification of the charging scheme, there is exactly one unit of charge per crossed non-red rectangle, we get that  $m_\chi \leq h_0 + 2m_0$ .  $\square$

In the recursive partitioning, we discard every one of the  $h_\chi + m_\chi$  rectangles that are crossed by vertical cut segments; what remains in the end are the  $h_0 + m_0$  rectangles that were not crossed and therefore not discarded. (These remaining rectangles either appear as isolated rectangles within a leaf face of the CCR-partition, or appear as special rectangles, which are penetrated but not crossed.) Now, Claim 5.8, together with the fact that  $m_0 + m_\chi \geq k/2$  (by assumption), imply that

$$h_0 + m_0 \geq m_\chi \geq (k/2) - m_0,$$

from which we see that

$$h_0 + 2m_0 \geq k/2,$$

and thus,

$$2(h_0 + m_0) \geq k/2.$$

This implies that

$$h_0 + m_0 \geq k/4,$$

which proves our main claim (with a 4-approximation),



**Claim 5.9.** *The total number,  $h_0 + m_0$ , of rectangles that are not crossed by vertical cut segments (and thus that survive) in the recursive partitioning is  $h_0 + m_0 \geq k/4$ .*

□

## An Improved Approximation Factor

While our main intention is simply to get an  $O(1)$ -approximation algorithm that runs in polynomial time, our method readily yields an improvement from a 4-approximation to a 3-approximation, with only a small change.

Our charging scheme above had slack in the fact that when we had a vertical segment portion,  $\sigma$ , of a cut cross one of the  $m_\chi$  non-red rectangles, we charged the rectangle in only *one* direction (to the right, in Figure 11). This source of slack came from just the few subcases in the proof of the technical lemma (case (3)(c) in the proof of Lemma 5.2) when it might be possible to require two vertical cut portions, whose projections onto the  $y$ -axis overlap. In particular, this led to our choice to assign charge in only one direction, left or right.

The simple modification we make is this: When a vertical cut segment  $\sigma$  crosses a non-red rectangle  $R$ , we charge this crossing in both directions (leftwards and rightwards), assigning a charge of  $1/2$  to each of the two charged corners (a northwest corner to the right of  $\sigma$  and a northeast corner to the left of  $\sigma$ ). This works fine in all cases (cases (1), (2), (3)(a), (3)(b) of Lemma 5.2) having a single vertical cut segment. Regarding case (3)(c), when we apply Lemma 5.2 to perform a cut in the proof of Theorem 3.1, if we are in case (3)(c), with two vertical cut portions having overlapping  $y$ -projections, we perform the cut in two parts, first cutting along one vertical segment  $\sigma_1$  (and its incident horizontal fence cuts), which results in a charging off of the crossed non-red rectangles and the establishment of associated new fences, and then performing the remainder of the cut, while taking into account the newly established fences. The fence invariant is maintained in this two-stage cut, resulting in partitioning of  $Q$  into a constant number (now, at most 6, instead of 5) subfaces, each being a CCR. Refer to Figure 12.

Since each rectangle having a corner that receives charge is charged at most once (its northwest corner or its northeast corner, Claim 5.7), we get that the total charge,  $m_\chi \leq (m_0 + h_0)/2$ , so that (using  $m_\chi + m_0 \geq k/2$ ) we get

$$(m_0 + h_0)/2 \geq m_\chi \geq (k/2) - m_0,$$

from which we see that

$$3m_0/2 + h_0/2 \geq k/2,$$

which implies that

$$3(m_0 + h_0) \geq k,$$

showing the 3-approximation.

**Modified Case (3)(c) in the proof of Lemma 5.2.** After the stage 1 cut, there could be new fences established anchored along the vertical cut segment  $\sigma_1$ . If none of these fences cross  $\sigma_2$ , then we complete the cut, along  $\sigma_2$  and the incident horizontal fence cut portions, as in the original case analysis. If, however, there is at least one new fence segment anchored on  $\sigma_1$ , extending leftwards across  $\sigma_2$ , then we let  $\beta'$  be that new fence segment extending leftmost (shown in purple in Figure 12). In this case, the stage 2 cut consists of a truncation of  $\sigma_2$  at  $\beta'$  (to yield a vertical cut segment  $\sigma_{2,1}$ ), together with a horizontal cut along  $\beta'$ , and a vertical cut segment  $\sigma_{2,2}$ , from the left endpoint of  $\beta'$  to the fence segment  $\alpha'$  (possibly  $\alpha' = \alpha^-$ ), and then along  $\alpha'$  to the left side  $\ell^-$ . (Note that vertical cut segments  $\sigma_{2,1}$  and  $\sigma_{2,2}$  have disjoint  $y$ -projections.)

## 6 Conclusion

Our main result is a first polynomial-time constant-factor approximation algorithm for maximum independent set for axis-aligned rectangles in the plane.

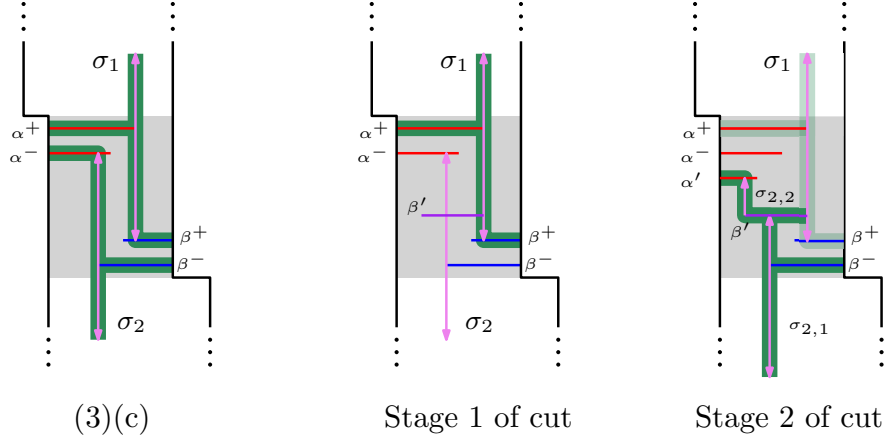


Figure 12: A modification to case (3)(c) in the proof of Lemma 5.2: When there are two vertical portions,  $\sigma_1$  and  $\sigma_2$ , in the cut, we perform  $\sigma_1$  first, potentially resulting in new fences segments anchored on  $\sigma_1$ , after which we perform the rest of the cutting into sub-face CCRs, modifying to account for the new fences. The subcase analysis is very similar to before, but we may now end up with at most 6 sub-faces (instead of 5). Here, we show only the portion of  $Q$  within the gray mid-rectangle; the subcases based on the interactions of the segments  $\sigma_1$  and  $\sigma_2$  with the fences and sides of  $Q$  in the L-shaped regions above and below the mid-rectangle are straightforward and unchanged from the description in the appendix (Figure 15).

Several open questions are topics for ongoing and future work. First, we are confident that, using methods introduced here, the approximation factor we obtain can be further improved; our goal here was to devise new methods that achieve a constant factor. We suspect that there is a more careful analysis of our charging scheme that will yield an improved factor, possibly to 2.5 or even better. More ambitiously, is there a PTAS? Our presented approach seems to give up at least a factor of 2 in its method of handling the nestedness issue, in order to guarantee enough rectangles can be charged to nearby rectangle corners; this may not be necessary, so there is hope that a PTAS will emerge from this work. Can the running time of a constant-factor approximation algorithm be improved significantly? Can the Pach-Tardos Conjecture 1 be resolved? (This would yield a constant-factor approximation algorithm with a significantly improved running time.)

Can our results be extended to the case of weighted rectangles in the plane, with the goal of maximizing the weight of an independent set? Do our methods extend to the case of independent sets of polygons more general than rectangles? What can be done in three or more dimensions, for MIS on hyperrectangles?

## Acknowledgements

I thank Mathieu Mari for his input on an earlier draft [19].

This work was partially supported by the National Science Foundation (CCF-2007275), the US-Israel Binational Science Foundation (BSF project 2016116), Sandia National Labs, and DARPA (Lagrange).

## Appendix

### Proof of Lemma 5.2

*Proof.* The proof is by a careful enumeration of cases.

All segments of all cuts are chosen to lie on the grid  $\mathcal{G}$  of vertical/horizontal lines through sides of the input rectangles. The figures show cases with CCRs that are most complex (12-sided); other cases of CCRs are simpler and are subsumed by the case analysis on the more complex CCRs. In particular, the simplest case is that in which the CCR  $Q$  is a rectangle, with no corners clipped, having sides labeled  $b$ ,  $t$ ,  $\ell$ , and  $r$

(bottom, top, left and right). Depending if a corner is clipped or not, there may or may not be sides  $b^-$ ,  $b^+$ ,  $t^-$ ,  $t^+$ ,  $\ell^-$ ,  $\ell^+$ , and  $r^-$ ,  $r^+$ .

In the figures below, the fences are shown in blue if their right endpoint lies on the right boundary (sides  $r^+$ ,  $r$ , or  $r^-$ ) of  $Q$ , and are referred to using the letter beta (“ $\beta$ ”); fences with left endpoint on the left boundary (sides  $\ell^+$ ,  $\ell$ , or  $\ell^-$ ) of  $Q$  are shown in red and are referred to using a letter alpha (“ $\alpha$ ”). (Note that a fence segment can extend from a (reflex) vertex of  $Q$ , as a collinear extension of one of the top/bottom sides  $t^-$ ,  $t^+$ ,  $b^-$ , or  $b^+$ .) For simplicity in the many figures, we omit showing the rectangles associated with each of the fences.

Only those fence segments that are needed to identify the subcases are shown; there may be numerous other red/blue fences. The fences that are shown in the figures are selected in a specific way, according to the case analysis, such as the fence extending furthest to the left/right, or the first fence hit by a vertical ray up/down from a fence endpoint, etc.

If there is a red fence segment that overlaps with a blue fence segment, then, together, these fence segments define a horizontal chord of  $Q$  that can serve as a CCR cut  $\chi$ , partitioning  $Q$  into two CCR subfaces. If there exists a vertical (grid) segment  $\sigma$  that does not cross any red/blue fences but that partitions  $Q$  into two subfaces (with one endpoint on  $t^-$ ,  $t$ , or  $t^+$ , and the other endpoint on  $b^-$ ,  $b$ , or  $b^+$ ), then  $\sigma$  constitutes a CCR-cut  $\chi$  of  $Q$  into two pieces, each of which is a CCR. The conditions (i)-(v) of the lemma hold.

If there are no rectangles of  $I'$  within  $Q$ , there are no fence segments, and the claimed statement is trivially true, as any vertical or horizontal cut along edges of the grid satisfies the claim, with the assumption that  $Q$  includes at least two rectangular grid faces. Thus, we assume that there is at least one fence segment; without loss of generality, we assume there is at least one blue fence segment, anchored on the right sides of  $Q$ . Let  $\bar{\beta}$  be a blue fence segment with leftmost left endpoint.

**Some notation.** We do a careful case analysis, with each case illustrated in the detailed figures. We use the following notation to indicate relationships among fence segments:

- We let  $\alpha \uparrow X$  (resp.,  $\alpha \downarrow X$ ) indicate that the upwards vertical ray from the right endpoint of the red fence segment  $\alpha$  first encounters feature  $X$ , with  $X$  being a top side of  $Q$  or another fence segment; in the figures, the portions of the corresponding rays are indicated with a pink directed segment (arrow). We similarly define the notation  $\alpha \downarrow X$  and, corresponding to up/down rays from the left endpoint of a blue fence segment  $\beta$ , the notation  $\beta \uparrow X$  and  $\beta \downarrow X$ .
- We let “ $\alpha \in X$ ”, for  $X \in \{\ell^-, \ell, \ell^+\}$ , denote the fact that the anchored (left) endpoint of red fence segment  $\alpha$  lies on the (left) side  $X$  of  $Q$ . We similarly use the notation “ $\beta \in X$ ”, for  $X \in \{r^-, r, r^+\}$ , according to which right side contains the right endpoint of a blue fence segment  $\beta$ .
- The cut  $\chi$  is indicated in the figures with thick green highlighting.

**The detailed case analysis.** Our case analysis is as follows:

- (1) [ $\bar{\beta} \in r$ ] We obtain subcases  $\bar{\beta} \uparrow X$  according to the choice of feature  $X \in \{t^-, t, t^+, \alpha\}$ , where  $\alpha$  is a potential red fence segment, with  $\alpha \in \{\ell^-, \ell, \ell^+\}$ . Refer to Figure 13.
  - (a) [ $\bar{\beta} \uparrow t^-, t$ ] We get a simple L-cut, which partitions  $Q$  into 2 CCR subfaces, as shown in the figure.
  - (b) [ $\bar{\beta} \uparrow t^+$ ] We cannot do a simple L-cut in this case, as one side would fail to be a CCR. Thus, we consider more complex cuts, with subcases  $\bar{\beta} \downarrow X$  according to the choice of feature  $X \in \{b^-, b, b^+, \alpha\}$ , where  $\alpha$  is a potential red fence segment, with  $\alpha \in \{\ell^-, \ell, \ell^+\}$ .
    - (i) [ $\bar{\beta} \downarrow b^-, b, b^+$ ] We get a T-cut, consisting of a single vertical cut segment and a single horizontal cut segment (along  $\bar{\beta}$ ), partitioning  $Q$  into 3 CCR subfaces.
    - (ii) [ $\bar{\beta} \downarrow \alpha \in \ell^-, \ell$ ] We get a cut that partitions  $Q$  into 3 CCR subfaces, as shown in the figures.
    - (iii) [ $\bar{\beta} \downarrow \alpha \in \ell^+$ ] In this case, we let  $\bar{\alpha}$  be the red fence anchored on  $\ell^+$ , at a point at or below  $\alpha$ , having a rightmost right endpoint. (Potentially,  $\bar{\alpha} = \alpha$ .) We know that  $\bar{\alpha} \uparrow \beta$ , for  $\beta$  a blue fence segment anchored on  $r$  or on  $r^-$ .

- (A)  $[\beta \in r^-]$  We consider subcases,  $\bar{\alpha} \downarrow X$ , according to the choice of  $X \in \{b^-, b, b^+, \alpha', \beta'\}$ .
  - (I)  $[\bar{\alpha} \downarrow b^-, b, b^+]$  We get a cut that partitions  $Q$  into 3 CCR subfaces, as shown in the figures.
  - (II)  $[\bar{\alpha} \downarrow \alpha' \in \ell^-, \ell]$  We get a cut that partitions  $Q$  into 3 CCR subfaces, as shown in the figures.
  - (III)  $[\bar{\alpha} \downarrow \beta' \in r^-, r]$  We get a cut that partitions  $Q$  into 3 CCR subfaces, as shown in the figures.
- (B)  $[\beta \in r^-]$  In this case, we define a *mid-rectangle*,  $W$ , whose  $y$ -extent is given by the overlap in  $y$ -coordinates between  $\ell^+$  and  $r^-$  and whose  $x$ -extent is from  $\ell^+$  to  $r^-$ ; in the figure, the mid-rectangle  $W$  is shown in gray. The fences  $\bar{\alpha}$  and  $\beta$  provide a witness to the fact that any vertical chord of the mid-rectangle  $W$  intersects a fence segment. We refer to this case as the *bridged mid-rectangle* case, and handle it separately below, in case (3).
- (c)  $[\bar{\beta} \uparrow \alpha \in \ell^-]$  In this case, we let  $\bar{\alpha}$  be the red fence anchored on  $\ell^-$ , at a point at or above  $\alpha$ , having a rightmost right endpoint. (Possibly,  $\bar{\alpha} = \alpha$ .) We know that  $\bar{\alpha} \downarrow \beta$ , for  $\beta$  a blue fence segment anchored on  $r$  or on  $r^+$ .
  - (i)  $[\beta \in r^-]$  We consider subcases depending on the feature that is above the right endpoint of  $\bar{\alpha}$ :
    - (A)  $[\bar{\alpha} \uparrow t^-, t, t^+]$  We get a cut that partitions  $Q$  into 3 CCR subfaces, as shown in the figures.
    - (B)  $[\bar{\alpha} \uparrow \alpha \in \ell, \ell^+]$  We get a cut that partitions  $Q$  into 3 CCR subfaces, as shown in the figures.
    - (C)  $[\bar{\alpha} \uparrow \beta' \in r, r^+]$  We get a cut that partitions  $Q$  into 3 CCR subfaces, as shown in the figures.
  - (ii)  $[\beta \in r^+]$  In this case, we get the bridged mid-rectangle case handled in case (3) below, since the fences  $\bar{\alpha}$  and  $\beta$  bridge the sides  $\ell^-$  and  $r^+$ . The bridged mid-rectangle  $W$  is shown in gray in the figure.
- (d)  $[\bar{\beta} \uparrow \alpha \in \ell, \ell^+]$  We get a Z-cut that partitions  $Q$  into 2 CCR subfaces, as shown in the figures.
- (2)  $[\bar{\beta} \in r^+]$  We obtain subcases  $\bar{\beta} \downarrow X$  according to the choice of feature  $X \in \{b^-, b, b^+, \alpha\}$ , where  $\alpha$  is a potential red fence segment, with  $\alpha \in \{\ell^-, \ell, \ell^+\}$ . Refer to Figure 14.
  - (a)  $[\bar{\beta} \downarrow b^-, b]$  We get a simple L-cut, which partitions  $Q$  into 2 CCR subfaces, as shown in the figure.
  - (b)  $[\bar{\beta} \downarrow b^+]$  We cannot do a simple L-cut in this case, as one side would fail to be a CCR. Thus, we consider more complex cuts, with subcases  $\bar{\beta} \uparrow X$  according to the choice of feature  $X \in \{t^-, t, \alpha\}$ , where  $\alpha$  is a potential red fence segment, with  $\alpha \in \{\ell^-, \ell, \ell^+\}$ . (Note that  $X = t^+$  is not possible, since  $\bar{\beta} \in r^+$ .)
    - (i)  $[\bar{\beta} \uparrow t^-, t]$  We get a T-cut, consisting of a single vertical cut segment and a single horizontal cut segment (along  $\bar{\beta}$ ), partitioning  $Q$  into 3 CCR subfaces.
    - (ii)  $[\bar{\beta} \uparrow \alpha \in \ell^-]$  In this case, we get the bridged mid-rectangle case handled in case (3) below, since the fences  $\bar{\beta}$  and  $\alpha$  bridge the sides  $\ell^-$  and  $r^+$ . The bridged mid-rectangle  $W$  is shown in gray in the figure.
    - (iii)  $[\bar{\beta} \uparrow \alpha \in \ell, \ell^+]$  We get a cut that partitions  $Q$  into 3 CCR subfaces, as shown in the figures.
  - (c)  $[\bar{\beta} \downarrow \alpha \in \ell^-, \ell]$  We get a Z-cut that partitions  $Q$  into 2 CCR subfaces, as shown in the figures.
  - (d)  $[\bar{\beta} \downarrow \alpha \in \ell^+]$  In this case, we define a rectangle,  $G$ , shown in light green in the figure, whose top side is  $t$  and whose vertical extent corresponds to the overlap in the  $y$ -coordinates of the sides  $\ell^+$  and  $r^+$ . In particular, in the shown figures for this case, the bottom endpoint of  $r^+$  lies below the bottom endpoint of  $\ell^+$ , so the bottom edge of  $G$  has left endpoint at the bottom endpoint of  $\ell^+$ ; the other case is symmetric, so is not shown separately. The fences  $\bar{\beta} \in \ell^+$  and  $\alpha \in \ell^+$  have overlapping  $x$ -projections; thus, when the set of all fences anchored on the left/right sides of the rectangle  $G$  are viewed from below, the lower envelope of these (horizontal) fence segments

within  $G$  has a transition from red to blue (going left to right), defined by a red fence  $\alpha^-$  and a blue fence  $\beta^-$ . Possibly  $\alpha^- = \alpha$ , and, independently, possibly  $\beta^- = \bar{\beta}$ . We either have then that  $\alpha^- \uparrow \beta^-$  (the case shown in the figures), or the case that  $\beta^- \uparrow \alpha^-$  (which is handled in exactly the same way, so is not separately shown here).

We now consider subcases  $\alpha^- \downarrow X$  according to the choice of feature  $X \in \{b^-, b, b^+, \alpha', \beta'\}$ , where  $\alpha'$  is a potential red fence segment, with  $\alpha' \in \{\ell^-, \ell\}$  ( $\alpha' \in \ell^+$  is not possible), and  $\beta'$  is a potential blue fence segment, with  $\beta' \in \{r^-, r, r^+\}$ .

- (i)  $[\alpha^- \downarrow b^-, b, b^+]$  We get a cut that partitions  $Q$  into 3 CCR subfaces, as shown in the figures. (Note that we included a horizontal cut segment along the full extent of  $\alpha^-$ ; for the cases  $\alpha^- \downarrow b^-, b$  this was optional and can be omitted, resulting in a partitioning of  $Q$  into just 2 CCR faces, one of which has the red fence segment  $\alpha^-$  extending fully across it from left side to right side.)
- (ii)  $[\alpha^- \downarrow \alpha' \in \ell^-, \ell]$  We get a cut that partitions  $Q$  into 3 CCR subfaces, as shown in the figures. (Again, we have included the optional cut along  $\alpha^-$ .)
- (iii)  $[\alpha^- \downarrow \beta' \in r^-, r]$  We get a Z-cut that partitions  $Q$  into 2 CCR subfaces, as shown in the figures.
- (iv)  $[\alpha^- \downarrow \beta' \in r^+]$  Let  $\bar{\beta}'$  be a blue fence anchored on  $r^+$ , at a point at or below  $\beta'$ , having a leftmost left endpoint. (Possibly,  $\bar{\beta}' = \beta'$ .) We partition into subcases below, depending on what features lie above/below the left endpoint of  $\bar{\beta}'$ . (Note that  $\bar{\beta}' \uparrow t^-$  is not possible (because of  $\bar{\beta}$ ),  $\bar{\beta}' \uparrow t$  is not possible (because it is blocked by fences), and  $\bar{\beta}' \uparrow \beta''$ , for a blue fence  $\beta''$ , is not possible (by definition of  $\bar{\beta}'$ .) We consider subcases  $\bar{\beta}' \downarrow X$ , according to the choice of feature  $X \in \{b^-, b, b^+, \beta'', \alpha''\}$ , where  $\beta''$  is a potential blue fence segment, with  $\beta'' \in \{r^-, r\}$  ( $\beta'' \in r^+$  is not possible, by the definition of  $\bar{\beta}'$ ), and  $\alpha''$  is a potential red fence segment, with  $\alpha'' \in \{\ell^-, \ell\}$  ( $\alpha'' \in \ell^+$  is not possible, since it must be below rectangle  $G$ ).
- (A)  $[\bar{\beta}' \downarrow b^-, b]$  We get a simple L-cut, which partitions  $Q$  into 2 CCR subfaces, as shown in the figures.
- (B)  $[\bar{\beta}' \downarrow b^+]$  We cannot do a simple L-cut in this case, as one side would fail to be a CCR. Thus, we consider more complex cuts, with subcases  $\bar{\beta} \uparrow \alpha'$ , where  $\alpha$  is a red fence segment, with  $\alpha \in \{\ell^-, \ell, \ell^+\}$ .
  - (I)  $[\bar{\beta}' \uparrow \alpha' \in \ell^-]$  In this case, we get the bridged mid-rectangle case handled in case (3) below, since the fences  $\bar{\beta}'$  and  $\alpha'$  bridge the sides  $\ell^-$  and  $r^+$ . The bridged mid-rectangle  $W$  is shown in gray in the figure.
  - (II)  $[\bar{\beta}' \uparrow \alpha' \in \ell, \ell^+]$  We get a cut that partitions  $Q$  into 3 CCR subfaces, as shown in the figures. (We have included the optional cut along  $\bar{\beta}'$ .)
- (C)  $[\bar{\beta}' \downarrow \beta'' \in r^-]$  We consider subcases  $\bar{\beta} \uparrow \alpha'$ , where  $\alpha'$  is a red fence segment, with  $\alpha' \in \{\ell^-, \ell, \ell^+\}$ .
  - (I)  $[\bar{\beta}' \uparrow \alpha' \in \ell^-]$  In this case, we get the bridged mid-rectangle case handled in case (3) below, since the fences  $\bar{\beta}'$  and  $\alpha'$  bridge the sides  $\ell^-$  and  $r^+$ . The bridged mid-rectangle  $W$  is shown in gray in the figure.
  - (II)  $[\bar{\beta}' \uparrow \alpha' \in \ell, \ell^+]$  We get a cut that partitions  $Q$  into 3 CCR subfaces, as shown in the figures. (We have included the optional cut along  $\bar{\beta}'$ .)
- (D)  $[\bar{\beta}' \downarrow \beta'' \in r]$  We consider subcases  $\bar{\beta} \uparrow \alpha'$ , where  $\alpha$  is a red fence segment, with  $\alpha \in \{\ell^-, \ell, \ell^+\}$ .
  - (I)  $[\bar{\beta}' \uparrow \alpha' \in \ell^-]$  In this case, we get the bridged mid-rectangle case handled in case (3) below, since the fences  $\bar{\beta}'$  and  $\alpha'$  bridge the sides  $\ell^-$  and  $r^+$ . The bridged mid-rectangle  $W$  is shown in gray in the figure.
  - (II)  $[\bar{\beta}' \uparrow \alpha' \in \ell, \ell^+]$  We get a cut that partitions  $Q$  into 3 CCR subfaces, as shown in the figures. (We have included the optional cut along  $\bar{\beta}'$ .)
- (E)  $[\bar{\beta}' \downarrow \alpha' \in \ell^-, \ell]$  We get a Z-cut that partitions  $Q$  into 2 CCR subfaces, as shown in the figures.

- (3) [**Bridged mid-rectangle** ] Assuming that  $\ell$  lies completely above  $r$  in  $y$ -coordinate, let the *mid-rectangle*,  $W$ , be the rectangle whose  $y$ -extent is given by the overlap in  $y$ -coordinates between  $\ell^-$  and  $r^+$  and whose  $x$ -extent is from  $\ell^-$  to  $r^+$ . The bridged mid-rectangle case assumes that any vertical chord of the mid-rectangle  $W$  intersects a fence segment. (There is a symmetric and equivalent case in which  $\ell$  lies completely below  $r$ , and the mid-rectangle  $W$  has  $y$ -extent given by the overlap in  $\ell^+$  and  $r^-$  and has  $x$ -extent from  $\ell^+$  to  $r^-$ .)

When viewed from above, the upper envelope of the fence segments within  $W$  has a transition from red to blue (going left to right), defined by a red fence  $\alpha^+$  and a blue fence  $\beta^+$ . Similarly, when viewed from below, the lower envelope of the fence segments within  $W$  has a transition from red to blue (going left to right), defined by a red fence  $\alpha^-$  and a blue fence  $\beta^-$ . Possibly  $\alpha^+ = \alpha^-$ , and, independently, possibly  $\beta^+ = \beta^-$ .

- (a) [ $\beta^+ \downarrow \alpha^+$  ] In this case, there is a Z-cut partitioning  $Q$  into 2 CCR subfaces.
- (b) [ $\alpha^- \uparrow \beta^-$  ] In this case, there is a Z-cut partitioning  $Q$  into 2 CCR subfaces.
- (c) [**Otherwise:**  $\alpha^+ \downarrow \beta^+$  **and**  $\beta^- \uparrow \alpha^-$  ] In this case, in addition to making a Z-cut along  $\alpha^+$  and  $\beta^+$  and the vertical transition segment linking the right endpoint of  $\alpha^+$  to  $\beta^+$ , we continue the vertical transition segment upwards, until it strikes  $t^-$ ,  $t$ ,  $\beta \in r^+$ , or  $\alpha \in \ell, \ell^+$ . (In the figures, the vertical transition segments are shown in pink.) Symmetrically, in addition to making a Z-cut along  $\alpha^-$  and  $\beta^-$  and the vertical transition segment linking the left endpoint of  $\beta^-$  to  $\alpha^-$ , we continue the vertical transition segment downwards, until it strikes  $b$ ,  $b^+$ ,  $\alpha \in \ell^-$ , or  $\beta \in r^-, r$ .
- Since the cases are all very similar and simple, in Figure 15 we illustrate just a few of the cases. (What makes the case analysis simple here is that the portion of  $Q$  above/below the mid-rectangle  $W$  is a very simple shape – a rectangle with just a *single* corner “clipped”.)

In all subcases, we obtain a partitioning of  $Q$  into 5 CCR subfaces.

**Observations and conclusion.** We summarize the results from the case analysis above with the following observations, in accordance with the parts (i)-(v) of the claims in the lemma:

- (i) In each case, the cut  $\chi$  partitions  $Q$  into at most 5 CCR subfaces. In most cases,  $Q$  is partitioned into 2 or 3 CCR subfaces; only in case (3)(c) can the number of CCR subfaces be as high as 5.
- (ii) In each case, the cut  $\chi$  is comprised of at most 2 vertical cut segments and at most 6 horizontal cut segments on the grid  $\mathcal{G}$ , with endpoints on the grid.
- (iii) In each case, the horizontal cut segments of  $\chi$  are a subset of the given red/blue anchored segments. Horizontal cut segments are either exactly equal to a fence segment or are equal to a subsegment of a fence segment that includes the fence segment’s anchored endpoint.
- (iv) In each case, the vertical cut segments of  $\chi$  do not cross any of the given red/blue anchored segments. In all cases, the vertical cut segments pass through an endpoint of a fence segment. The endpoints of each vertical cut segment lie either on the boundary of  $Q$  (a top/bottom side of  $Q$ ) or on fence segments (either at an endpoint of the fence or at a point interior to the fence).
- (v) In all cases except (3)(c), there is a single vertical cut segment; in case (3)(c) there are two vertical cut segments.

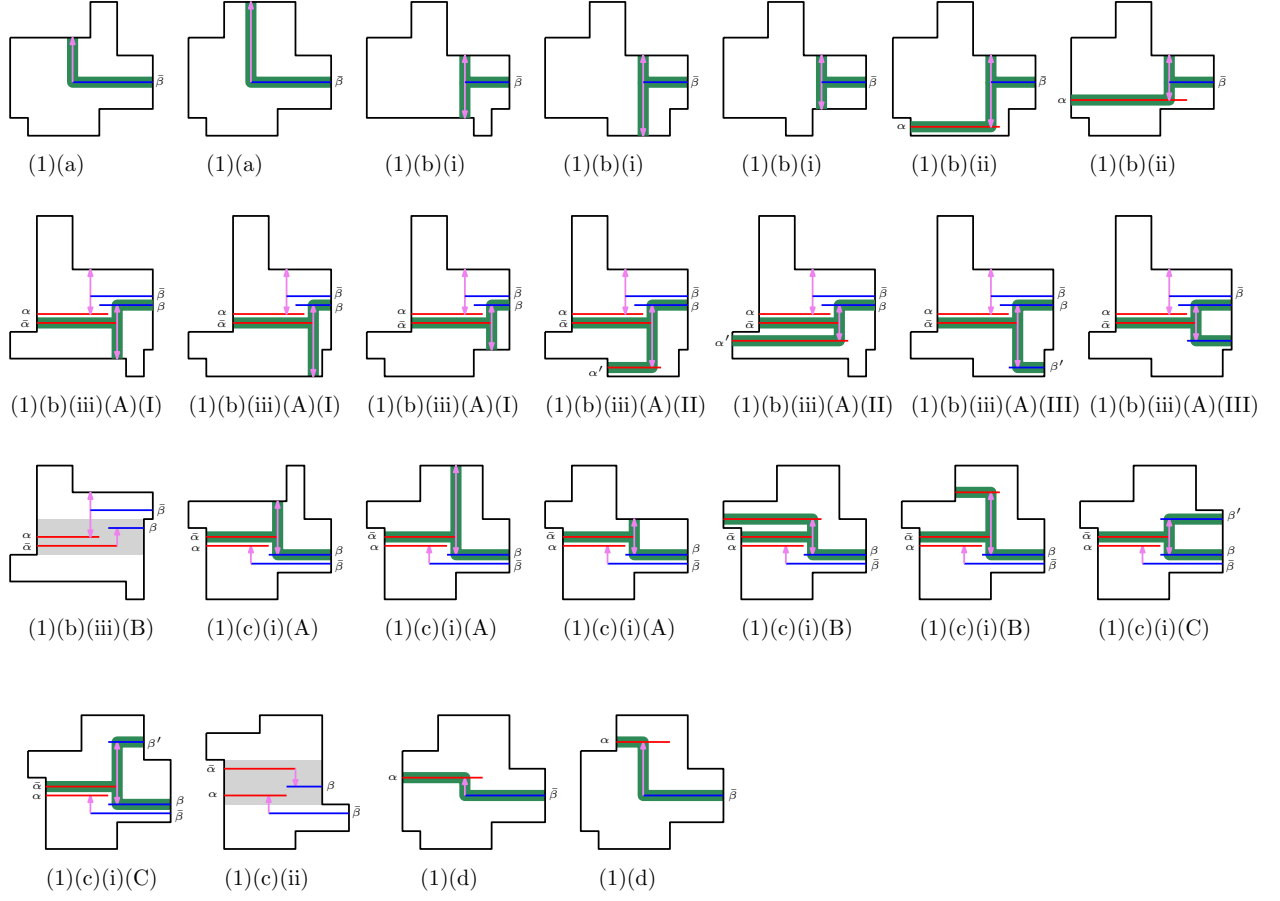
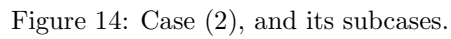


Figure 13: Case (1), and its subcases.





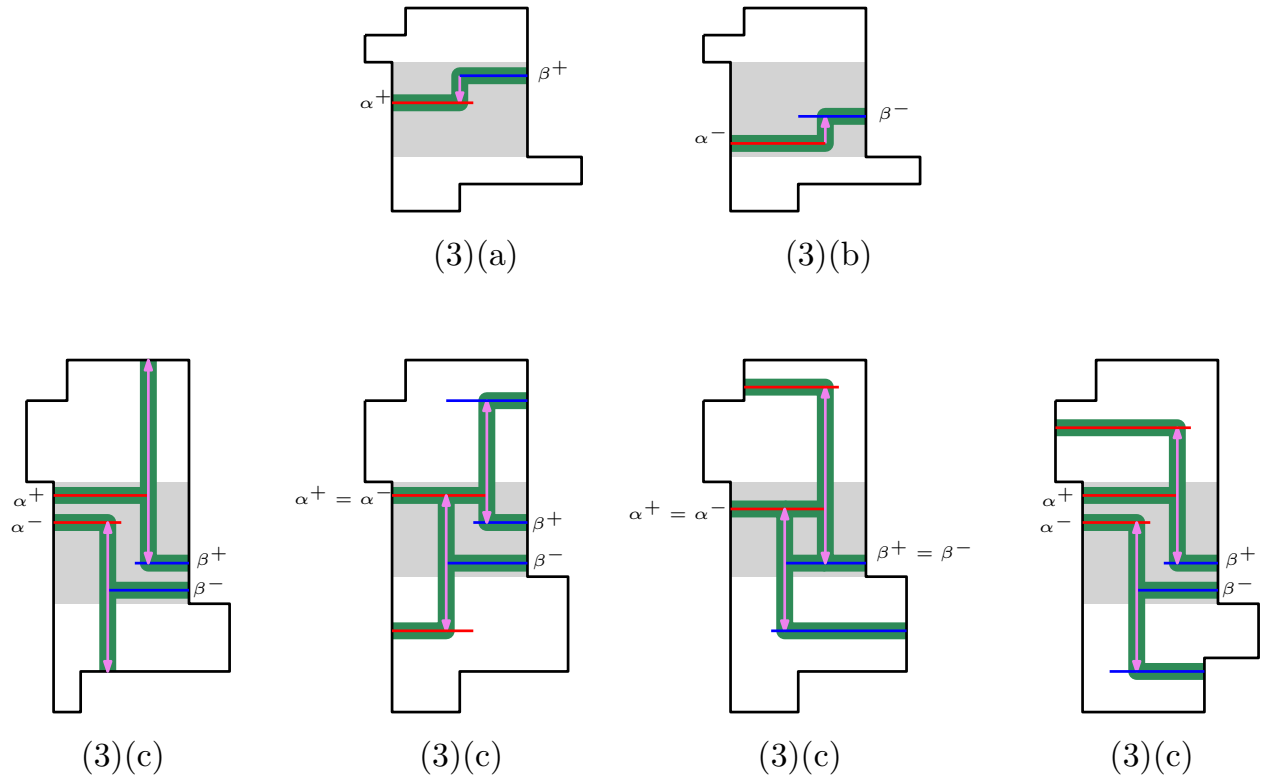


Figure 15: Case (3), and its subcases.

## References

- [1] Anna Adamaszek, Sarel Har-Peled, and Andreas Wiese. Approximation schemes for independent set and sparse subsets of polygons. *Journal of the ACM (JACM)*, 66(4):29, 2019.
- [2] Anna Adamaszek and Andreas Wiese. Approximation schemes for maximum weight independent set of rectangles. In *2013 IEEE 54th Annual Symposium on Foundations of Computer Science*, pages 400–409. IEEE, 2013.
- [3] Anna Adamaszek and Andreas Wiese. A QPTAS for maximum weight independent set of polygons with polylogarithmically many vertices. In *Proceedings 25th Annual ACM-SIAM Symposium on Discrete Algorithms*, pages 645–656. SIAM, 2014.
- [4] Pankaj K Agarwal, Marc van Kreveld, and Subhash Suri. Label placement by maximum independent set in rectangles. *Computational Geometry: Theory and Applications*, 3(11):209–218, 1998.
- [5] Piotr Berman, Bhaskar DasGupta, Shanmugavelayutham Muthukrishnan, and Suneeta Ramaswami. Improved approximation algorithms for rectangle tiling and packing. In *Proceedings 12th Annual ACM-SIAM Symposium on Discrete Algorithms*, volume 7, pages 427–436, 2001.
- [6] Ravi Boppana and Magnús M Halldórsson. Approximating maximum independent sets by excluding subgraphs. *BIT Numerical Mathematics*, 32(2):180–196, 1992.
- [7] Parinya Chalermsook. Coloring and maximum independent set of rectangles. In Leslie Ann Goldberg, Klaus Jansen, R. Ravi, and José D. P. Rolim, editors, *Approximation, Randomization, and Combinatorial Optimization. Algorithms and Techniques*, pages 123–134, Berlin, Heidelberg, 2011. Springer Berlin Heidelberg.
- [8] Parinya Chalermsook and Julia Chuzhoy. Maximum independent set of rectangles. In *Proceedings 20th Annual ACM-SIAM Symposium on Discrete Algorithms*, pages 892–901. Society for Industrial and Applied Mathematics, 2009.
- [9] Julia Chuzhoy and Alina Ene. On approximating maximum independent set of rectangles. In *2016 IEEE 57th Annual Symposium on Foundations of Computer Science (FOCS)*, pages 820–829. IEEE, 2016.
- [10] Mark De Berg, Marko M de Groot, and Mark H Overmars. Perfect binary space partitions. *Computational geometry*, 7(1-2):81–91, 1997.
- [11] Thomas Erlebach, Klaus Jansen, and Eike Seidel. Polynomial-time approximation schemes for geometric intersection graphs. *SIAM Journal on Computing*, 34(6):1302–1323, 2005.
- [12] Robert J Fowler, Michael S Paterson, and Steven L Tanimoto. Optimal packing and covering in the plane are np-complete. *Information processing letters*, 12(3):133–137, 1981.
- [13] Jacob Fox and János Pach. Computing the independence number of intersection graphs. In *Proceedings 22nd Annual ACM-SIAM Symposium on Discrete Algorithms*, pages 1161–1165. SIAM, 2011.
- [14] Fabrizio Grandoni, Stefan Kratsch, and Andreas Wiese. Parameterized approximation schemes for independent set of rectangles and geometric knapsack. *arXiv preprint arXiv:1906.10982*, 2019.
- [15] Sarel Har-Peled. Quasi-polynomial time approximation scheme for sparse subsets of polygons. In *Proceedings Annual Symposium on Computational Geometry*, pages 120–129, 2014.
- [16] Hiroshi Imai and Takao Asano. Finding the connected components and a maximum clique of an intersection graph of rectangles in the plane. *Journal of Algorithms*, 4(4):310–323, 1983.

- [17] J. Mark Keil, Joseph S.B. Mitchell, Dinabandhu Pradhan, and Martin Vatshelle. An algorithm for the maximum weight independent set problem on outerstring graphs. *Computational Geometry: Theory and Applications*, 60:19–25, 2017. Special issue devoted to selected papers from CCCG 2015. URL: <http://www.sciencedirect.com/science/article/pii/S092577211630044X>.
- [18] Sanjeev Khanna, S. Muthukrishnan, and Paterson Mike. On approximating rectangle tiling and packing. In *Proceedings 9th Annual ACM-SIAM Symposium on Discrete Algorithms*, volume 95, page 384. SIAM, 1998.
- [19] Joseph S. B. Mitchell. Approximating maximum independent set for rectangles in the plane. *CoRR*, abs/2101.00326, January, 2021.
- [20] Frank Nielsen. Fast stabbing of boxes in high dimensions. *Theoretical Computer Science*, 246(1-2):53–72, 2000.
- [21] David Zuckerman. Linear degree extractors and the inapproximability of max clique and chromatic number. *Theory of Computing*, 3:103–128, 2007.

□